

NASA Technical Memorandum 4084

Flight Test Experience and Controlled Impact of a Remotely Piloted Jet Transport Aircraft

Timothy W. Horton and Robert W. Kempel

NOVEMBER 1988

(NASA-TM-4084) FLIGHT TEST EXPERIENCE AND
CONTROLLED IMPACT OF A REMOTELY PILOTTED JET
TRANSPORT AIRCRAFT (NASA) 44 p CSCL 01b

NO 4-10 11

THE LIB

11/05 010760

NASA

NASA Technical Memorandum 4084

**Flight Test Experience
and Controlled Impact
of a Remotely Piloted
Jet Transport Aircraft**

Timothy W. Horton and Robert W. Kempel
*Ames Research Center
Dryden Flight Research Facility
Edwards, California*



National Aeronautics
and Space Administration

Scientific and Technical
Information Division

1988

CONTENTS

ABSTRACT	1
INTRODUCTION	1
NOMENCLATURE	2
Subscripts:	3
TEST OBJECTIVES	3
AIRPLANE DESCRIPTION AND FLIGHT TEST PROCEDURE	4
Airplane	4
Flight Test Procedure	4
REMOTELY PILOTED VEHICLE SYSTEMS	5
Ground Systems	5
Decommuration station.	5
Remotely piloted vehicle pilot's station.	5
Control law computers.	6
Uplink encoder.	6
Airborne Systems	6
Uplink receiving and decoding.	6
Uplink interface box and relay box	6
PB-20D autopilot.	7
Throttle system	7
Landing gear	7
Flap system	7
Brakes and nosewheel steering	8
Engine kill system	8
Terminate system.	8
CONTROL SYSTEMS	9
Pitch Control System	9
Roll Control System	9
Yaw Control System	9
Nosewheel Steering System	9
Throttle and Autothrottle Systems	10
Brake System	10
In-Flight Remotely Piloted Vehicle System Engagement	10
GUIDANCE SYSTEMS	10
General Guidance Configuration	10
Data Processing Requirements	11
Lateral Racetrack Guidance Control Law	12
Lateral Final Approach Guidance Control Law	12
Longitudinal Racetrack and Final Approach Guidance Control Law	13
PILOTED TEST FLIGHTS	13

IMPACT FLIGHT REMOTELY PILOTED VEHICLE RESULTS	16
Impact Conditions	17
Results and Analysis of Impact Flight Approach	17
Region A	17
Region B	17
Region C	17
Region D	17
CONCLUDING REMARKS	19
APPENDIX — LONGITUDINAL FINAL APPROACH GUIDANCE	
CONTROL LAW CALCULATIONS	20
REFERENCES	21

ABSTRACT

The Dryden Flight Research Facility of NASA Ames Research Center (Ames-Dryden) and the Federal Aviation Administration conducted the controlled impact demonstration (CID) program using a large, four-engine, remotely piloted jet transport airplane. Closed-loop primary flight was controlled through the existing onboard PB-20D autopilot which had been modified for the CID program. Uplink commands were sent from a ground-based cockpit and digital computer in conjunction with an up-down telemetry link. These uplink commands were received aboard the airplane and transferred through uplink interface systems to the modified PB-20D autopilot. Both proportional and discrete commands were produced by the ground system. Prior to flight tests, extensive simulation was conducted during the development of ground-based digital control laws. The control laws included primary control, secondary control, and racetrack and final approach guidance. Extensive ground checks were performed on all remotely piloted systems; however, piloted flight tests were the primary method of verification and validation of control law concepts developed from simulation. The design, development, and flight testing of control laws and systems required to accomplish the remotely piloted mission are discussed.

INTRODUCTION

The National Aeronautics and Space Administration (NASA) and the Federal Aviation Administration (FAA) conducted a joint program for the acquisition, demonstration, and validation of technology for the improvement of transport aircraft occupant crash survivability using a large, four-engine, remotely piloted transport airplane in a controlled impact demonstration (CID) (Kempel and Horton, 1985). The CID program was conducted at the Dryden Flight Research Facility of NASA Ames Research Center (Ames-Dryden), at Edwards, California, and was completed in late 1984. The objectives of the CID program were (1) to demonstrate a reduction of postcrash fire through the use of antimisting fuel (Klueg, 1985), (2) to acquire transport crash structural data (Hayduk and Alfaro-Bou, 1985), and (3) to demonstrate the effectiveness of existing improved seat-restraint and cabin structural systems (Hayduk and Alfaro-Bou, 1985).

The airplane used in the CID program, a four-engine B-720 jet transport manufactured in the early 1960s, typifies jet transport aircraft of that era. This airplane was nearing the end of its useful life when it was transferred to NASA by the FAA for conduct of the CID program.

The crash scenario was to be representative of a survivable accident, such as could occur following a missed approach or takeoff abort. The precise requirements of the antimisting kerosene (AMK) and crashworthiness experiments of the CID mission dictated tight constraints on impact parameters such as airspeed, sink rate, pitch angle, and impact location.

Ames-Dryden, with its unique facilities, capabilities, and extensive remotely piloted vehicle (RPV) experience, was selected to

1. prepare the test airplane and associated experiments for the final mission,
2. design and implement all RPV systems,
3. conduct all manned RPV checkout test flights, and
4. conduct the final impact mission.

The authors discuss the design, development, and flight testing of the systems required to accomplish the remotely piloted mission and present a summary of the final mission.

NOMENCLATURE

ADI	attitude direction indicator
AGL	aboveground level
AMK	antimisting kerosene
CID	controlled impact demonstration
CSMC	computer select mode control
d	distance from racetrack, ft
EGT	exhaust gas temperature
EPR	engine pressure ratio
FAA	Federal Aviation Administration
h	altitude, ft
HUD	head-up display
ILS	instrument landing system
K	system gain
MLS	microwave landing system
MSL	mean sea level
NASA	National Aeronautics and Space Administration
PCM	pulse code modulation
RPM	revolution per minute
RPV	remotely piloted vehicle
r	yaw rate in deg/sec or rad
s	laplace transform operator
SIBLINC	scale, invert, bias, logic, interface console
T_{\max}	autopilot elevator servo model maximum allowable torque
V	airspeed, knots

X	downrange position, n. mi. or ft
Y	lateral distance from centerline, n. mi. or ft
γ	flight path angle, deg or rad
ζ	damping ratio
θ	pitch angle, deg or rad
ϕ	bank angle, deg or rad
ψ	heading angle, deg or rad
ω	frequency, rad/sec

Subscripts:

aimpt	aimpoint
cas	calibrated airspeed
cmd	command
err	error
radar	calculated from radar data
ref	reference value
rwy	final approach coordinate system
T	racetrack coordinate system

TEST OBJECTIVES

The airspeed, sink rate, and pitch angle were selected to maintain fuselage integrity during acquisition of longitudinal and vertical acceleration data. Combining all of the CID experiment requirements into one flight resulted in a desired set of impact conditions as follows:

1. Velocity (ground speed), knots	152.5 ± 2.5
2. Rate of sink, ft/sec	17 ± 1
3. Pitch angle, deg	1 ± 1
4. Bank angle, deg	0 ± 2
5. Heading (relative to impact runway heading), deg	0 ± 2
6. Lateral displacement (Y), ft	0 ± 15
7. Longitudinal displacement (X), ft	0 ± 75

It was further specified that the impact would be with the landing gear in the retracted position, flaps at 30° , and a maximum amount of fuel would be carried.

Predetermined program ground rules dictated that above an altitude of 400 ft above ground level (AGL), any of the specified major experimenters could call a mission abort or go-around if their equipment suffered a major failure, and below 400 ft, only the project pilot could call an abort or go-around. Below 150 ft the airplane was committed to impact, because below this altitude a go-around attempt might result in impact with the ground.

The layout of the crash site is shown in figure 1. The triangular obstacles are wing cutters, designed to open wing fuel tanks to ensure dispersal of AMK. The heavy horizontal line was a fence 8 ft high, made of frangible material to aid the RPV pilot in the targetting task. Where the runway centerline intersects the fence, a bright orange panel was placed to provide the RPV pilot with a visual guidance aimpoint.

AIRPLANE DESCRIPTION AND FLIGHT TEST PROCEDURE

Airplane

The B-720 airplane is a swept-wing, swept-tail, four engine medium-range jet transport. The CID B-720 aircraft is shown in figure 2 in a practice go-around. The lines on the fuselage were used to measure fuselage deformation during the final impact. The principal physical dimensions of the B-720 airplane are shown in figure 3. The approximate empty weight was 98,000 lb with a structural design gross weight of 203,000 lb. The gross weight at takeoff for the impact flight was 200,500 lb.

Extensive modifications were required to convert the airplane from a piloted (crew of three) to a remotely piloted vehicle (RPV) while retaining the piloted capability of the crew for RPV checkout. Instrumentation was added to support each of the various experiments and the RPV systems.

Primary flight controls were ailerons, elevator, and rudder. The ailerons and elevator were controlled by aerodynamic tabs and assisted by aerodynamic balance panels. The rudder was hydraulically powered and assisted by aerodynamic balance panels; however, a manually operated aerodynamic tab backup was provided.

The outboard ailerons were designed to stay in the faired position with the flaps retracted and then to operate with increasing authority as a function of increasing flap deflection. Upper wing surface spoilers augment roll control with the inboard ailerons and also operate as speed brakes. Double slotted flaps and leading edge flaps provide lift and drag control for slow-speed flight.

Pitch trim was through a variable incidence stabilizer. Roll and yaw trim were operated through aileron and rudder, respectively.

For the CID program, the existing PB-20D autopilot (Federal Aviation Administration, 1970) was modified and used to operate as the primary RPV flight control. Unused portions of the autopilot were deactivated as a part of the modification for remote-piloted operation to eliminate potential failure points.

Flight Test Procedure

The primary approach in checking out the B-720 RPV systems was piloted flight tests. Both the onboard pilot and copilot could disengage all RPV system functions with a disengage switch on their cockpit control wheel.

Prior to the final CID mission, a total of 14 piloted test flights was made, as well as 10 remote takeoffs, 13 remote landings, and 69 CID approaches. All remote takeoffs with crews aboard were flown from the Edwards main runway with the remote landings on an emergency recovery lakebed runway.

The actual CID mission profile and boundary are presented in figure 4. The takeoff runway was lakebed runway 17 on Rogers Dry Lake. Following takeoff the vehicle would make a gentle left-hand turn until it intersected the oval racetrack pattern at approximately 2300 ft AGL which was 4600 ft mean sea level (MSL). With the airplane

level and on the racetrack, a right turn with a radius of 1.4 n. mi. was performed with a rollout on the impact runway heading. Final approach glideslope guidance was initiated at the heading intercept point approximately 5.6 n. mi. from the impact point.

If the final mission had to be aborted, the emergency recovery runway (runway 25) at the south edge of the lakebed would have been used to recover the aircraft.

The terminate boundary is shown as the light boundary on the outside of the buffer (darker) boundary (fig. 4). If for any reason the aircraft strayed outside the buffer boundary, a terminate command would be transmitted through an independent uplink system. The terminate signal commanded full nose down stabilizer, rudder right, engine fuel shut off, and gear down to ensure that the vehicle would impact within the sterile area indicated by the terminate boundary.

REMOTELY PILOTED VEHICLE SYSTEMS

During RPV checkout flights with the crew, flight crew safety was of primary concern. Therefore, it was necessary that the remotely piloted capability be developed while ensuring the integrity of the conventional onboard piloted control system. The existing autopilot was capable of receiving instrument landing system (ILS) radio signal command inputs to the elevator and aileron channels. Replacing the ILS radio signal command paths with uplinked elevator and aileron command signals provided the basic RPV capability. Rudder pedal commands were added to the basic parallel yaw damper. The autopilot retained its attitude-hold feedback paths so that only uplink commands from the ground were required, that is, no feedback paths from the airplane were required to be closed on the ground. Both proportional and discrete commands had to be implemented from the ground station. Primary pitch, roll, and yaw commands, as well as the throttle and brakes, were proportional while flaps, engine fuel shutoff, landing gear up-down, nosewheel steering left-right, and emergency brakes were discrete commands. The ground system was primarily dual channel for increased reliability; however, some less critical elements were single channel. The airborne system was simplex or single-channel, again, because of the mentioned constraints. The uplink command path and the downlink telemetry signals are shown in figure 5.

The single-string airborne system was used because a flight crew would be aboard during RPV testing, and the crew would assume command in the event of any RPV anomalies. Once checked out, the unmanned mission would be relatively short in duration, thereby minimizing exposure time. Providing redundancy in the RPV systems onboard the B-720 aircraft was considered beyond the scope of the program because of time and monetary constraints.

Ground Systems

Flight test instrumentation data were transmitted to the ground as a pulse code modulation (PCM) data stream. Each parameter was sampled at 200 Hz (Harney and others, 1985). The ground station received and decommutated the data into usable data words in counts. The ground RPV system is shown in figure 6. From this figure it can be seen that the ground systems were divided into active and standby (or A and B, respectively) systems. The simplex elements in this system included the pilot's control stick computer and the relay box that selected the redundant systems. The SIBLINC (the hardware interface between computer and cockpit) was also simplex.

Decommutation station. The decommutation computer formatted data from the vehicle sensor signals and combined this information with the formatted ground-based radar data. These data were then transferred to the control law computer for additional processing.

Remotely piloted vehicle pilot's station. The RPV pilot in the ground cockpit is shown in figure 7, while the general cockpit layout and instrument array are shown in figure 8. Cockpit instrument displays included two forward-looking video receivers (one color and one black-and-white), attitude direction indicator (ADI), radar altimeter, and airspeed, altitude rate, engine revolutions per minute (RPM), fuel flow, exhaust gas temperature (EGT), and engine pressure ratio (EPR) indicators.

The ground pilot's controls consisted of conventional stick and rudder pedals for aircraft three-axis proportional control. A stick computer allowed stick and rudder characteristics, such as breakout force, force gradient, limits, and trim rates, to be selected by the project pilot to obtain desirable handling qualities. The interface from the pilot's controls to the control law computers was through the stick computer for the active system or the SIBLINK for the standby system. A proportional throttle, physically similar to the four throttle controls aboard the B-720 aircraft was also provided; however, only a single throttle command was transmitted to the aircraft because the onboard throttle handles had been linked together to move as one unit.

Discrete controls included landing gear up-down, flaps up-down, nosewheel steering left-right, individual engine kill, and individual fire bottle discharge. Proportional brakes were provided as toe brakes on the rudder pedals.

Control law computers. The two control law computers contained the ground-to-air control laws, as well as guidance algorithms. The code in both computers was identical. The pilot's stick and rudder pedal commands were output from the stick computer to the active control law computer. These commands were also passed to the SIBLINC and transferred to the standby control law computer. Most of the discrete commands were passed through the SIBLINC to both the active and standby computers as were the active proportional throttle and brake commands. Switching from active to standby systems was automatic only if the active control law computer failed, otherwise the pilot handled fault detection and switching.

Uplink encoder. The command signals were output from either the active or standby control law computers to identical uplink encoders. The uplink encoders were formatted to transmit 16 16-bit words per frame at a rate of 40 frames per sec. The system was designed so that 16 words were available; however, the CID required only 9 words for data transmission. The first 10 bits of each word contained a proportional channel and the last 6 bits were discrete commands. The uplink data format is shown in figure 9. The proportional channels represented the interface to the vehicle aerodynamic control surfaces, throttle, and brakes. These signals were then uplinked to the aircraft via either the primary triplex antenna or backup communications antenna. The triplex and communications antennas were manually selected in the ground pilot's cockpit.

Airborne Systems

Uplink receiving and decoding. The airborne RPV system is shown in figure 10. The uplink receiving and decoding system consisted of dual antennas, dual receivers, a signal combiner, and an uplink decoder. The signal combiner continuously combined the output signals of the dual receivers so that regardless of the orientation of the aircraft with respect to the transmitting antenna, the best signal was available for all uplink commands.

Uplink interface box and relay box. The interface box provided the signal interface between the uplinked signals and the airplane systems. These signals were received as digital signals and output as analog signals for the proportional commands and as relay driver signals for the discrete commands. Discrete commands went to the uplink relay box, providing signals to the flaps, nosewheel steering, emergency pneumatic brakes, landing gear, engine kill, and fire bottles. Analog commands included main brakes, throttle, and autopilot. For flight crew safety during piloted flight tests, the command signals to the emergency brakes and engine kill functions were physically

disconnected. Each of the other functions could be disengaged by the autopilot disengage switch action by either the B-720 pilot or copilot. The autopilot disengage switch was on the pilot and copilot's control wheel.

PB-20D autopilot. The variable mode PB-20D autopilot was modified to receive the uplink pitch, roll, and yaw ground commands. The glide slope-auto mode was designed so that ILS analog radio signals were the input commands to the elevator (glide slope) and aileron (localizer). Therefore, this mode was selected to receive the uplinked pitch and roll commands with a rudder command added to complete the three-axis control.

The basic feedback paths of the autopilot included pitch attitude and pitch rate in the pitch channel, bank angle and roll rate in the roll channel, and yaw rate in the rudder channel. These feedback paths were retained for the RPV system; however, the pitch forward loop gain was modified for the CID program to provide acceptable airplane response when flying through ground effect (Curry and Bowers, 1985). This gain modification will be discussed in more detail in the Piloted Test Flights section.

A variety of other modifications to the autopilot was required for the CID program: these changes included bypassing all automatic disengage functions. These disengage functions could be activated by either fault detection or erroneous engage procedures. However, for the piloted RPV test flights, the three-phase power monitor and pilot-copilot emergency autopilot disengage functions were retained. Unused or deactivated electronic components were physically removed to simplify the autopilot and eliminate as many potential failure points as possible.

The rudder channel was not a primary autopilot channel in that the yaw damper was operational as part of normal autopilot operation but no command path existed. Therefore, the rudder uplink command channel was added to the autopilot.

Manually adjustable potentiometers were added on the pitch, roll, and yaw command inputs as part of the uplink signal conditioning. Flight tests then were conducted to determine the potentiometer settings required to ensure acceptable signal gain of the ground-generated commands. The rudder channel also required the addition of a modulator downstream of the potentiometer to convert the dc signal to the appropriate ac signal for the autopilot. The pitch and roll channels used their existing modulators.

Throttle system. The B-720 aircraft had an existing limited authority autothrottle connected by clutches to all four throttles. This system was modified to receive the single uplinked proportional throttle command.

Landing gear. Complete remote actuation of the landing gear was required in the CID program. Since the landing gear of the B-720 aircraft was controlled by raising and lowering the cockpit landing gear lever, it was decided that the simplest method to control the gear from the ground would be to physically move the landing gear lever rather than parallel the existing functions for RPV operation. A small dc motor was installed which actuated a cable assembly and moved the landing gear lever in either direction as required. On-off limit switches were installed at the full-up and full-down lever positions. Discrete ground commands for gear up or down were received in the uplink relay box, which activated relays that controlled the motor direction, thus lowering or raising the landing gear as required.

Flap system. The remote flap actuation system was electrically tied to the aircraft emergency flap system. The RPV flap system was mechanized into the three emergency flap switches aboard the aircraft. These switches were

1. hydraulic bypass on-off switch,
2. inboard flap electric motor, and

3. outboard flap electric motor.

Three discrete commands from the ground actuated the flaps. These discrete commands were actuated from two switches in the ground cockpit. The discrete commands were

1. flap bypass hydraulics,
2. flap up, and
3. flap down.

The ground RPV flap enable switch in the off position represented the flap bypass off and resulted in the flaps remaining in the position selected by the B-720 cockpit flap lever. With this switch in the on position the flaps could be repositioned, using the up-down or off switch, via the electric motors rather than the normal hydraulics.

Brakes and nosewheel steering. An RPV brake system was required for engine run-up and for landings. The RPV brake system was mechanized in the B-720 aircraft by installation of left and right brake control valves actuated by a pulse command based on a proportional uplink command for left or right braking from 0 to 100 percent.

The nosewheel steering system was mechanized using relay logic, a dc motor, and a pulley cable assembly. In the RPV mode, the nosewheel limit was $\pm 10^\circ$.

The emergency brake system was also part of the RPV system and was mechanized so that a single discrete from the ground would lock the brakes. For piloted flights, this system was disabled to ensure that no stray signal could inadvertently activate the system.

Engine kill system. The normal individual engine kill and fire bottle discharge system was mechanized so that a ground discrete could activate either system. Once either action was initiated, however, it could not be reversed.

Terminate system. An independent terminate system was installed aboard the B-720 aircraft to ensure that the aircraft would not pose a threat to populated areas in the event of any RPV control system failure. This system was designed to be isolated, as much as possible, from the onboard B-720 flight control systems. Activation of the termination system resulted in the following actions onboard the aircraft:

1. Engine 1, 3, and 4 fuel valves were commanded to the off position immediately. To retain aircraft electric and hydraulic power, the number 2 engine was programmed to shut down 25 sec later.
2. Emergency pneumatic brakes were activated.
3. Landing gear was lowered.
4. Throttles were moved to the idle position.
5. Stabilizer was commanded to the maximum leading edge up (nose down) position.
6. Rudder was commanded to full nose right.

Once the terminate command was issued, it was irreversible. The terminate system was demonstrated during ground tests, but was never active during piloted flights. During piloted flights, the system was wired to a test box where a series of lights would illuminate to give a positive indication that the system operated as specified.

CONTROL SYSTEMS

The following control systems are represented as continuous systems using the Laplace transform variable "s" representation. All systems were mechanized for analysis in a ground-based digital computer with all appropriate sampled data transformations being made. The mechanization of the autopilot, shown in figures 11 to 13 and figure 16, represents a modified version as it was used in the CID program and mechanized in the simulation. All of the block diagrams in the figures represent the systems in their final configuration.

Pitch Control System

The control laws for the pitch axis are shown in figure 11. The RPV pilot commands pitch attitude of the B-720 airplane by movement of a control stick in the ground-based cockpit. A pitch attitude command that was proportional to stick deflection was sent to the pitch axis of the PB-20D autopilot. Full stick deflection of ± 4 in. commanded -12 deg to $+15$ deg of pitch attitude. A pitch trim button on the RPV pilot's stick moved the stick at a constant rate of 2.9° of pitch attitude command per sec.

Figure 11 also shows how the autopilot processed the uplink attitude command. The signal was summed with pitch angle and pitch rate feedbacks and with a turn compensation term. The autopilot sent a command to the autopilot servo, which in turn deflected the control surface through a tab-elevator system. An autotrim command was also created to drive the stabilizer to reduce the elevator servo loads.

The autopilot elevator servo model used on the simulator is shown in figure 12. This model was developed from a comparison of simulation and flight step responses (see Piloted Test Flights section).

Roll Control System

The ground-based and onboard autopilot control laws for the roll axis are shown in figure 13. Gain schedules in figure 13 are shown in figures 14 and 15. Early in the program, the RPV pilot chose an attitude command system, rather than rate command, for primary control in the roll axis. The RPV pilot commanded roll attitude of the aircraft proportional to the lateral displacement of the control stick in the ground-based cockpit. The pilot inputs went through a small deadband (0.9°) and produced commands that were uplinked to the roll axis of the onboard autopilot. Full deflection of the roll stick (± 4 in.) commanded $\pm 35^\circ$ of bank angle.

Yaw Control System

The RPV pilot commanded rudder deflection to the B-720 aircraft through the yaw damper. The RPV rudder control system is shown in figure 16. The rudder pedal position signal was passed through a deadband, and a rudder command proportional to pedal deflection was uplinked to the airplane. Full rudder pedal commanded $\pm 25^\circ$ of rudder deflection.

Nosewheel Steering System

Uplink discrettes commanded the nose wheel left or right via the ground cockpit rudder pedals. A nosewheel enable-disable switch was provided in the ground cockpit.

A diagram representing the implementation of the ground-based cockpit's nosewheel steering system is also shown in figure 16. The RPV pilot generated a nosewheel position command that was proportional to rudder pedal displacement when the nosewheel steering was engaged. This command was then compared to the downlinked nosewheel servo position command. A nose-left or nose-right discrete command was uplinked to the onboard RPV

nosewheel steering system motor. This motor then drove the nosewheel servo command. A limit cycle resulted from the delay in the feedback through the downlink system. A deadband in the pilot command loop was used to reduce the magnitude of this limit cycle. The amount of deadband necessary was determined from actual system use (see Piloted Test Flights section).

Throttle and Autothrottle Systems

The RPV pilot commanded the throttle to the airplane through a single lever in the RPV cockpit. An autothrottle was provided in the ground-based software to free the RPV pilot from making throttle adjustments during flight. The mechanization of the ground cockpit throttle system, the autothrottle implementation, and the simulation model of the engine dynamics are shown in the figure 17. The throttle was limited to a range between 68 percent engine rpm (idle) and maximum throttle.

The autothrottle was engaged to hold indicated airspeed at a prespecified value. A reference airspeed of 146 knots was determined from simulation to give the desired true airspeed of 152.5 knots at impact, after passing through ground effect (Curry and Bowers, 1985). The autothrottle controlled the downlinked, onboard-computed airspeed (V_{cas}). This downlinked airspeed was compared to the reference airspeed to produce an airspeed error. This error signal was passed through a proportional and an integral path. The integrator was initialized at the current value of the pilot throttle lever position and was limited to a -50 to $+75$ percent range to prevent saturation if the autothrottle was engaged at an airspeed that was significantly different than the reference speed. A filtered pitch angle term was used to lead the throttles when the flightpath was changed. The autothrottle command was limited to a range of 0 to 75 percent (approximately maximum continuous thrust). This command was uplinked to the B-720 throttle system.

Brake System

The ground cockpit had toe brakes in the rudder pedal system. The RPV pilot could command 0 to 100 percent left or right brake by deflecting the appropriate brake pedal. The proportional brake commands were then uplinked to the onboard brake system.

In-Flight Remotely Piloted Vehicle System Engagement

During the piloted test flights, it was necessary to engage the uplink system for test purposes without incurring significant transients. Pitch transients were reduced by adjusting the longitudinal stick position until the commanded pitch attitude was equal to the actual pitch attitude using an RPV cockpit display of the error between these two parameters. The pitch attitude error was displayed on the pitch flight director bar when the pitch trim engage button was selected. The throttle transients were similarly reduced by comparing the downlinked throttle position to the uplink throttle command. The throttle error was displayed on the glideslope error bug when the throttle trim engage button was selected. Roll transients were reduced by centering the lateral stick and engaging the RPV system with wings level. The pitch trim system is shown in figure 11. The throttle trim is shown in figure 17.

GUIDANCE SYSTEMS

General Guidance Configuration

Two modes of guidance were provided to aid the RPV pilot in flying the B-720 aircraft. One mode, the racetrack guidance, assisted the pilot in flying the racetrack pattern. The second mode, final approach guidance, assisted

the RPV pilot in flying either of two possible final approach patterns. The final approach patterns was either to the abort runway (runway 25) or to the impact runway. The final approach guidance aided the pilot in flying the desired approach path and attaining the desired conditions at touchdown or impact. The reference point for all guidance calculations was the desired impact point on the lakebed. The coordinates of this point were determined using the NASA FPS-16 radar, and all computations were based on coordinates relative to this point. Guidance input parameters were determined in the ground-based computer using a combination of radar data and downlinked airplane data. The four parameters determined for each of the coordinate systems were the downrange position X and the lateral distance from centerline Y ground positions, the altitude h , and the heading angle ψ .

The racetrack and final approach (impact runway) patterns are shown in figure 18. A coordinate system was established for each of the final approach runways and for the racetrack.

Three guidance mode options were available, as follows:

1. Racetrack, in which only the racetrack guidance was used;
2. Final approach, where only the final approach was used; and
3. Automatic, in which the racetrack and final approach modes were selected automatically depending on location of the aircraft.

Guidance mode and runway were selected in the RPV cockpit.

In the simulation development of the guidance systems, many of the actual elements involved were only approximated or not modeled at all, including the following:

1. Manual tracking of the B-720 aircraft by the radar operator was not modeled. (Automatic radar tracking was found to be unacceptable due to the negative elevation angles required between the radar site and the impact point.)
2. Refraction of the radar beam by the atmosphere was not modeled.
3. Precession of the gyros onboard the B-720 aircraft were not modeled.
4. The visual scene presented to the RPV pilot was not like the actual television picture from the airplane but was a computer-generated series of raster lines that approximated the runway image and did not represent a real world image. This image, although synthetic, was clearer than the actual video out-the-nose view in flight.

Data Processing Requirements

Prior to computation of the guidance laws, it was found that the aircraft position data supplied by the tracking radar required enhancement to determine a more accurate estimate of its actual position in space. Two sources of data were required to determine the guidance computations. The first source was actual aircraft state data (except position) downlinked from onboard the B-720 aircraft, and, the second, airplane position and position rate data supplied by the NASA FPS-16 tracking radar system. These data were then combined in an algorithm for the determination of position and heading for use in the guidance control laws. The specific problem with using only radar data, which was supplied by the tracking station, for guidance was the time lag introduced by filtering (to smooth the radar data) in the supplied signal. This time lag resulted in unacceptable real time guidance computations.

To improve the quality of the required guidance parameters (position and heading), the downlinked data from the airplane were combined with the radar data (figs. 19(a) through 19(d)) to produce an improved estimate of the actual values. The objective of these computations was to combine the high-frequency information contained

in the downlinked data with the low-frequency information from the radar. The general procedure was to use the downlinked data to determine the rate-of-change of the required guidance parameters, integrate the parameters, compare these results with the radar-supplied steady-state parameters, and then correct the integration for any biases. The radar data also required the addition of a lead term to compensate for radar-filtering time lag. The heading was calculated (fig. 19(a)) whenever the guidance was selected and was displayed to the pilot in addition to being used in the guidance calculations. The downrange position X , (fig. 19(b)), the altitude h , (fig. 19(c)), and the lateral distance from centerline Y , (fig. 19(d)), were made only in the final approach mode and were used only in the guidance calculations. The lateral distance calculation required a double integration since the downlinked data provided acceleration rather than rate information. The output from these computations was then used as the input to the appropriate guidance control law.

The following table shows the data, its source, and relationship to various guidance modes:

Parameter	Lateral		Longitudinal
	Racetrack	Final	Both
Radar derived			
X , ft	X	X	X
Y , ft	X	X	X
X dot, ft/sec		X	
Y dot, ft/sec		X	
H , ft		X	X
ψ , rad	X	X	
PCM downlink			
ϕ , deg	X	X	
yaw rate, deg/sec	X	X	
altitude rate, ft/sec			X

Lateral Racetrack Guidance Control Law

The lateral racetrack guidance control law provided lateral guidance to the RPV pilot in the form of a fly-to flight director needle. Raw position information, in the form of lateral distance from the centerline relative to the racetrack, was also presented to the ground pilot on the localizer bug in the RPV cockpit. Full scale was ± 400 ft of lateral distance error in the racetrack mode. The flight director needles and bugs are shown in figure 20. The guidance was designed to lead the pilot to the racetrack and to provide appropriate commands to maintain the racetrack pattern.

Implementation of the racetrack lateral guidance laws is shown in figure 21. The needle command that the pilot saw on the roll needle was a bank angle command. This command was made up of a command proportional to the distance from the track, a heading command owing to the difference between the aircraft heading and the heading of a tangent to the racetrack, and, if in the turn portion of the racetrack, a command to maintain a coordinated turn.

Lateral Final Approach Guidance Control Law

The final approach lateral control law provided information to the RPV pilot by means of fly-to flight director needles as well as raw displacement from the centerline information. Again, the guidance command was seen on the lateral flight director needle, and the raw centerline error was displayed on the localizer bug of the ground cockpit. Full scale on the raw data varied linearly from 400 feet of error at or above an altitude of 1700 ft, to 60 ft at and below 500 ft.

The final approach lateral guidance laws are shown in figure 22. The centerline error was summed with its rate to produce a heading command. The airplane heading angle and heading angle rate were combined to form a heading

error which was then transformed into a bank angle error. This attitude error became a roll command which drove the RPV pilot's lateral flight director needle.

Longitudinal Racetrack and Final Approach Guidance Control Law

The longitudinal guidance control law provided flight director and raw displacement information for both the racetrack and the final approach modes. The raw information was altitude above or below the reference altitude, which was the altitude of the racetrack, or the altitude on the desired glideslope. This error was displayed on the glideslope error bug in the RPV cockpit. Full scale varied linearly from ± 200 ft at 2000 ft AGL, to ± 50 ft at 1000 ft AGL.

Guidance laws for the longitudinal axis are shown in figure 23. For the final approach mode, the reference altitude and the actual altitude are compared, generating an altitude error. For the racetrack mode, the altitude error was the vertical distance from the racetrack altitude of 4600 ft MSL. The altitude error was then summed with an altitude rate error that was obtained by comparing the actual and reference altitude rates. The sum of the altitude rate and altitude error terms becomes a pitch flight director command that was displayed to the RPV pilot on his pitch flight director needle.

The automatic switching from the racetrack to the final approach mode was based on the location of the B-720 aircraft on the racetrack. The location for switching from racetrack to final approach guidance was chosen to minimize the transient motion of the pitch flight director command needle. Detailed calculations for the longitudinal final approach guidance can be found in the appendix of this report.

PILOTED TEST FLIGHTS

Piloted flight tests of the B-720 airplane provided the means by which available theoretical mathematical models for simulation, RPV control laws, RPV support software, and RPV hardware were verified for the CID mission. In addition, the aerodynamic effects of the vehicle in close proximity to the ground were determined. Major benefits of the piloted flight tests were the assessment of RPV handling qualities and numerous practice CID approaches and emergency landings.

Early in the program, management realized that to achieve the CID mission, a valid engineering simulation would be required as a mission trainer and to assist in systems development. Mathematical models of the aircraft aerodynamics, autopilot, flight control system, and engines were available. However, certain system gains and dynamic elements were poorly defined or not defined at all. Therefore, the early flight tests were necessary to acquire data to improve the data base for further systems development.

Once the simulation models were updated by the use of flight data, control laws could be validated and verified.

The piloted flights also allowed testing of all onboard systems of the B-720 aircraft. These systems included engine degraders (used to prepare the AMK fuel for burning in the engines), autopilot, brakes, landing gear, nosewheel steering, and instrumentation systems.

There was little flight experience with the engine degraders prior to the CID program and limited experience with the AMK fuel. The degraders were modified as a result of the CID flight tests.

Emergency procedures also were tested during the piloted test flights. These procedures included the ability to land the B-720 airplane on the lakebed abort runway under RPV control, and partial testing, in flight, of the uplinked termination system.

For the acquisition of flight data, step input commands were mechanized in the ground-based computer. These step inputs were controlled in both amplitude and time duration, and were input to the elevator, ailerons, and rudder.

These step commands were uplinked to the airborne autopilot in place of the normal, ground-pilot control commands. The aircraft responses to the pulses were downlinked and recorded in the ground station for postflight analysis. The flight responses then were compared to pulse response data from the simulation, and simulator gains and dynamic elements were modified until the simulation results matched the flight response.

From the flight test results, it was determined that the yaw step response matched that of the simulation very well, but pitch and roll responses did not match the simulator results. The flight results indicated that the autopilot pitch gain and the equivalent elevator servo dynamics, as modeled, were in error. The pitch gain problem was traced to an incorrectly grounded autopilot isolation amplifier. After this amplifier was properly grounded, the actual pitch gain matched that of the simulation. To fully match the flight response, the simulation elevator servo dynamics were modified from a first-order model to that shown in figure 12. The torque limit of the autopilot servo provided a rate limit, and, in conjunction with the torque feedback from the tab position, provided a position limit that was a function of airspeed. The servo model torque limit was determined from a match of flight test data so that the elevator response was limited to the flight value by the predicted torque required. A time delay was added to the servo model to produce the overall stability of the closed-loop autopilot-servo-elevator system as seen from the flight data. Modifications to the simulator resulted in closer correlations between data from actual flight and those of the simulator.

The roll response showed that the onboard gain was higher than anticipated, saturating the system. The autopilot gain was lowered, a good match was obtained, and the lateral handling qualities were improved.

To determine the dynamic response of the engines, the autothrottle was engaged at an airspeed different than the reference airspeed, resulting in a step input to the system. It was determined that the engines responded faster than the initial simulation model. The faster responding engines were equivalent to having higher gains in the autothrottle, resulting in oscillatory behavior during flight. An engine's fuel-flow response to the step autothrottle maneuver for the original simulation engine model is shown in figure 24. The figure also shows the actual response seen on flight 1. The flight response was then matched on the simulator by modifying the model of the engine dynamics. This is shown in the third plot of figure 24. The fourth engine response plot (fig. 24) shows the simulation response after the engine model was revised, and after the autothrottle control laws were modified. The autothrottle performed exceptionally well in flight after the ground control laws were modified in response to the flight test results.

The guidance systems that were designed to aid the RPV pilot during the final mission were also tested during the test flights. Some gains in the various systems were varied as a result of flight experience, including the scaling gains that scaled the guidance information on the RPV pilot displays.

The design of the guidance systems was continually being modified to accommodate the comments of the RPV pilot.

Flight time for guidance development was limited because of the program schedule, as was RPV pilot time with the final guidance configuration.

RPV taxiing of the B-720 airplane for piloted test flights allowed observation of the RPV nosewheel steering system performance. Limit cycle oscillations of the nosewheel were observed when the RPV nosewheel steering was used. The system was designed with command deadbands to reduce these limit cycles. Once the limit cycles were seen during taxi, the values of the deadbands in the ground software were changed to reduce the oscillations.

Flight test also allowed testing of a new uplink-downlink system and testing of the onboard autopilot hardware. During the 14 piloted test flights, four problems were encountered within the RPV uplink system, interfaces, and autopilot. These four anomalies occurred on four different flights. In all cases, the instrumentation available was insufficient to determine the exact cause.

These four anomalies can be stated briefly as follows:

1. Intermittent loss of RPV uplink signal for approximately 60 sec;
2. Apparent loss of pitch autopilot command inputs from 28 to 41 sec (two intervals of time);
3. Failure of uplink decoder to pass uplink commands for an extended interval following a flight, with the B-720 airplane on the ground;
4. Uncommanded 9° left roll in the RPV mode while making a landing approach.

The first three anomalies called for modifications that were implemented based on suspected causes. In each case, the anomaly never recurred. The fourth was traced to the autopilot, but could not be duplicated and the problem never recurred.

The corrective action for the intermittent loss of the RPV uplink signal can be described as follows: the signal combiner was equipped with a dual output capability, but only one output channel was required for the CID program. The second channel was not being used. Therefore, it was decided that the uplink monitor could be installed on this unused channel. Afterwards, no further losses in uplink signal were experienced.

The corrective action taken for the second listed anomaly was the replacement and interchanging of certain autopilot components. An uplink card replacement corrected the third anomaly.

Observing these problems during the piloted test flights allowed corrective actions to be made prior to the unmanned impact flight. These anomalies could have compromised achieving the CID program impact goals had they occurred at the wrong time on the final flight.

Early simulation results indicated that the impact point, sink rate, and vehicle pitch attitude were highly dependent on the ground effect model with specific autopilot gains. To ensure that the specified impact conditions would be met, a series of flight tests were conducted to verify the B-720 ground effects. The problem was that the B-720 aircraft had a positive lift increment and nose-down pitching moment due to ground effect. With no control system, the airplane would pitch down, losing more lift due to reduction of angle of attack than the increase gained in ground effect and would impact short of the target. With a high autopilot pitch gain, the airplane would maintain attitude and impact beyond the target. Therefore, it was necessary to verify the aircraft's ground effect and adjust the autopilot pitch gain to ensure that the lift loss from the decrease in angle of attack matched the lift increase due to ground effect. As a result of the flight tests, it was determined that the increment of lift increase caused by ground effect was significantly larger than had been predicted, while the nose-down pitching moment was about as predicted (Curry and Bowers, 1985). The result of these tests was a reduction in the autopilot inner loop gain by 62 percent to that shown in figure 11.

All RPV takeoffs and landings were generally satisfactory, although the landings proved to be a difficult piloting task. The difficulty was a result of poor depth perception and lack of peripheral vision through the out-the-nose video monitor. The poor depth perception was caused, in part, by the use of a standard, low resolution, 525-line monitor.

The flight tests showed the CID mission to be a high-workload task for the RPV pilot. One contributing factor to the high workload was the FPS-16 tracking radar used in the guidance systems. This radar lacked the accuracy necessary to be used in a guidance system designed to meet such constrained impact parameters.

The accuracy of the radar used in the guidance systems was subject to the following problems:

1. manual optical tracking of the airplane,
2. large distance (about 7 miles) between the radar and the airplane,
3. negative elevation angle,

4. atmospheric diffraction over this distance, and
5. possibility of radar reflections.

The radar accuracy problem can be illustrated by the fact that, prior to flight 11, the radar measured the range to the impact site reference stake as 38,458 ft, and prior to flight 12, the same measurement was found to be 38,435 ft. This discrepancy of 23 ft was greater than the allowable lateral error of 15 ft.

Experience with FPS-16 tracking radar-driven guidance from previous Ames-Dryden programs existed at the beginning of the CID program; however, the requirements for CID were much more demanding in terms of accuracy. The radar appeared adequate to drive the guidance at the beginning of the CID program.

During the flight tests certain attempts were made to improve the performance of the RPV pilot. These changes included the following:

1. The length of the descent from the racetrack to impact was increased by relocating the racetrack to the position shown in figure 4. This relocation gave the RPV pilot more time to line up on the approach centerline during the final approach.
2. The length of the centerline oil strip at the impact site was increased to aid the RPV pilot in lining up on the centerline.
3. The landing lights along the impact runway were turned on.
4. All oil strip markings at the target site were recoiled prior to the impact flight to give maximum contrast between the lakebed and impact runway.
5. A black target fence, made of frangible material, was placed perpendicular to the long approach tar strip. Where the fence intersected the centerline, a bright orange target panel was emplaced on the fence. It was also thought that the 8-ft high fence would give a vertical reference to the RPV pilot.

All of these attempts to improve the performance of the RPV pilot were compromised by the use of the low-resolution video monitor.

During the 14 piloted test flights, 16 hr and 22 min of RPV control was accumulated, 10 RPV takeoffs were made, 69 RPV controlled approaches to the CID site with go-around at 200 ft were flown, and 13 RPV landings on the abort runway 25 were performed.

IMPACT FLIGHT REMOTELY PILOTED VEHICLE RESULTS

The final CID flight was made on December 1, 1984. Figure 25 shows the B-720 aircraft approaching the impact site during the last flight. Figure 26 shows the actual impact, while figure 27 shows the slideout of the airplane after impact. During the impact flight, some of the desired impact conditions were not achieved. The events that occurred during the final approach and an evaluation of the significance of these events on the impact conditions that were achieved are reviewed as follows. The analysis is based on recorded downlink parameters and on the radar and computer-generated guidance information.

Impact Conditions

The actual impact conditions compared to the design goals are summarized in the following table:

	Design goals	Impact
1. Velocity (ground speed), knots	152.5 ± 2.5	151.5
2. Rate of sink, ft/sec	17 ± 1	17.4
3. Pitch angle, deg	1 ± 1	-0.25
4. Bank angle, deg	0 ± 2	-12
5. Heading, deg	0 ± 2	1.5
6. Lateral displacement (Y), ft	0 ± 15	+20 (right)
7. Longitudinal displacement (X), ft	0 ± 75	-282 (short)

The longitudinal and lateral displacement values listed are those of the fuselage impact, rather than the initial left-engine and left-wingtip impact.

Results and Analysis of Impact Flight Approach

Some of the pertinent lateral-directional parameters near impact are shown in figure 28, and the longitudinal parameters are shown in figure 29. The time histories are broken into four regions (A to D), based on lateral activity, as shown in the figures.

Region A. The lateral activity in region A, which was typical of the entire approach up to this point, consisted of fairly regular pulsing of the stick commanding a right bank. This was required to offset the small bank angle bias of the onboard gyro. This bank angle bias had been a problem on previous flights and resulted from gyro precession during the turn followed by a very slow gyro erection time. The lateral deviation had drifted to about a 30 ft error at the end of region A. Based on simulator runs, this magnitude of error would be acceptable since it was relatively easy to reduce to the allowable 15 ft tolerance in a steady-state manner in the time remaining.

Region B. In region B, the RPV pilot stopped making any significant lateral corrections for about 10 sec while he was working the longitudinal task since the altitude error was increasing significantly immediately before region B and was reduced to an acceptable level by the end of the region. It could have also been caused, in part, from the need to change between the video display and the cockpit instruments to cross-check the validity of the guidance information. Whatever the reason, in this period without any pilot inputs, the roll bias produced a left turn (about a 2° bank). This, in turn, caused the lateral deviation to start moving rapidly to the left (rapidly in terms of the 15 ft constraint). The actual crossrange drift rate was about 3 ft/sec at the end of region B.

Region C. In region C, with the longitudinal problem in hand, the pilot became aware of the lateral motion to the left and began correcting with several right bank commands. The drift to the left was stopped and reversed, resulting in the airplane moving equally rapidly toward the right and ending with about a 30 ft error to the right by the end of region C.

Region D. At this point, the go-around decision point of 150 ft AGL had been reached. Just prior to this decision point, the airplane was slightly to the right of the centerline and a go-around was considered by the pilot, but it appeared that sufficient altitude remained to maneuver back to the centerline. With this assessment coupled with the concern about the lack of redundancy in the overall system, the pilot decided to continue the approach. At about 100 ft a fairly sharp, left lateral command was initiated to correct the lateral offset error accompanied by a pushover to ensure that the airplane did not overshoot the target area. The left lateral command initiated a lateral oscillation that did not have time to damp prior to impact. Depth perception through the video was poor, and it was difficult to accurately judge where the touchdown would occur. The aggressive lateral piloting technique used in region D did arrest the diverging lateral error. However, this did not occur within the desired range and produced relatively large bank angles, resulting in a significant bank angle at impact.

In the pitch axis, the pitch attitude was held within the desired range (0 to 2°) during this final region, although it was oscillating. The pitch command was oscillatory and diverging. The altitude error was converging on the desired value until the large bank angles occurred. At this point, altitude was lost due to a slight pushover (about 1°) and the lift loss caused by the banking, resulting in the impact short of the desired point.

During most of the project development period, simulation was performed without wind or turbulence models. The impact flight was to be flown only in calm conditions. Simulation indicated that the project pilot had a high probability of meeting all desired impact conditions.

Flight experience showed a larger dispersal of parameters around the desired values at the 200 ft go-around point than predicted by the simulation. The parameters were well within the range that the pilot could correct during the remaining time until impact. The RPV pilot commented that the airplane was more difficult to fly than the simulator.

In the final months prior to the impact flight, wind and turbulence models were incorporated in the simulation. After these modifications were in place, further simulation tests showed the probability of meeting the desired impact conditions were favorable, but adversely affected by even light turbulence. The pilot noted that with these added complications, the simulation had become more difficult to fly than the actual airplane.

Winds measured approximately at the time of impact indicated a headwind of 2 knots and a starboard crosswind of 3 knots relative to the impact runway heading at 200 ft AGL.

The requirement of having to impact under such tight constraints, together with the 3-knot crosswind during the final approach, contributed to the difficulty of the task for the RPV pilot. It was also difficult for the RPV pilot to integrate all the information presented and then to manually adjust the flightpath to meet all of the desired conditions. The controls design team generally agreed that some form of head-up display should have been used in the CID program, and that more of the piloting tasks should have been automated.

This analysis indicates that the desired impact conditions were not met as precisely as desired because of two related factors:

1. A bank angle bias that could produce significant turn rates if unattended; and
2. A high workload task that did not allow continuous monitoring of both the pitch and roll axes. A primary contribution to the workload was the need to integrate data from the cockpit instruments and the video information. The RPV pilot was also saturated by too much information, which contributed to the high workload of the task. He had to monitor the out-the-nose video information, as well as the instrument panel guidance information. None of these sources alone provided consistent, accurate guidance information, so the RPV pilot had to integrate all pieces of information, and, at the same time, control the B-720 aircraft. The pilot also had to visually scan between the monitor and the instrument panel to see all of the available information.

These factors, when taken together, created a dynamic situation that made it difficult to reach the impact conditions in as smooth and accurate a manner as was desired.

Although not all impact parameters were within the desired tolerances, most of them were. The effects of the conditions that were not met varied among the different experiments.

CONCLUDING REMARKS

The remotely controlled impact demonstration program was undertaken to acquire data that would contribute to the technology for the improvement of transport aircraft occupant crash survivability. The B-720 transport used in this test was modified to be flown remotely from the ground using the onboard PB-20D autopilot as primary control. Simulation was used to design the remotely controlled systems which were verified and validated in flight tests. Extensive flight tests were performed to practice the impact scenario. However, the impact site was never approached below an altitude of 150 ft.

During the flight tests, it was realized that the tracking radar data used in the guidance were not accurate enough for the task. Therefore, relying on the guidance alone was inadequate. Better guidance information could have been obtained by using a microwave landing system (MLS), rather than the tracking radar.

The CID impact piloting task was a higher workload task than the flight test RPV landings because of the tight impact constraints. The final mission proved to be a particularly high workload task because of the requirement to integrate all of the information presented to the RPV pilot. After the impact flight, the controls design team generally agreed that some form of head-up display (HUD) should have been used and that more of the piloting tasks should have been automated. These features could have improved the guidance if more accurate information could have been provided by a microwave landing system.

As a result of the high workload task, not all of the impact parameters were met; however, from a remotely piloted aspect, all ground and airborne systems performed as specified.

Although not all impact conditions were met, the aircraft impacted in the general area of the target, and remained in the target area during slideout. In addition, all RPV systems performed as specified. Therefore, from a remotely piloted vehicle standpoint, the program was considered a success.

*Ames Research Center
Dryden Flight Research Facility
National Aeronautics and Space Administration
Edwards, California, December 17, 1987.*

APPENDIX — LONGITUDINAL FINAL APPROACH GUIDANCE CONTROL LAW CALCULATIONS

For the final approach mode, the reference glide slope γ_{ref} , and the reference altitude are defined from the reference altitude rate (17.0 ft/sec) and the reference velocity (152.5 knots = 257.3 ft/sec), and are calculated as follows:

$$\begin{aligned}\dot{h}_{\text{ref}} &= -17.0 \text{ ft/sec} \\ \gamma_{\text{ref}} &= \sin^{-1}(\dot{h}_{\text{ref}}/V_{\text{ref}}) = \sin^{-1}(-17.0/257.3) \\ &= -0.0661 \text{ rad} = -3.79^\circ \\ h_{\text{ref}} &= -X_{\text{rwy}} * \tan |\delta_{\text{ref}}| \\ (h_{\text{ref}} &= 0.0 \text{ when } X_{\text{rwy}} > 0.0)\end{aligned}$$

The reference altitude from mean sea level (MSL) for the racetrack was dependent on the runway selected, 4600 ft for the impact runway and 4000 ft for abort runway.

The altitude aboveground level was calculated from the radar altitude and the aimpoint altitude. The aimpoint altitude was the MSL altitude of the aimpoint on the selected runway, and the nominal value was defined as follows for the two runways:

$$\begin{aligned}\text{crash runway} - h_{\text{aimpt}} &= 2275 \text{ ft} \\ \text{abort runway 25} - h_{\text{aimpt}} &= 2300 \text{ ft}\end{aligned}$$

There was a provision for entering the aimpoint altitude of the crash runway on the day of the flight based on radar measurements made at that time.

REFERENCES

Kempel, R.W., and T.W. Horton, *Flight Test Experience and Controlled Impact of a Large, Four-Engine, Remotely Piloted Airplane*, NASA TM-86738, 1985.

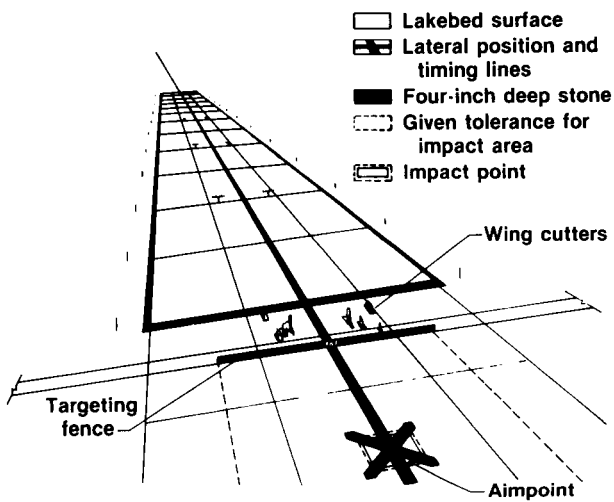
Klueg, E.P., *Antimisting Fuel Technology for Transport Category Aircraft*, SAE Technical Paper 851886, 1985.

Hayduk, R.J., Emilio Alfaro-Bou, and E.L. Fasanella, *NASA Experiments Onboard the Controlled Impact Demonstration*, SAE Technical Paper 851885, 1985.

Federal Aviation Administration, *Boeing 720 Operations Manual*, Department of Transportation, Federal Aviation Administration, Nov. 1970.

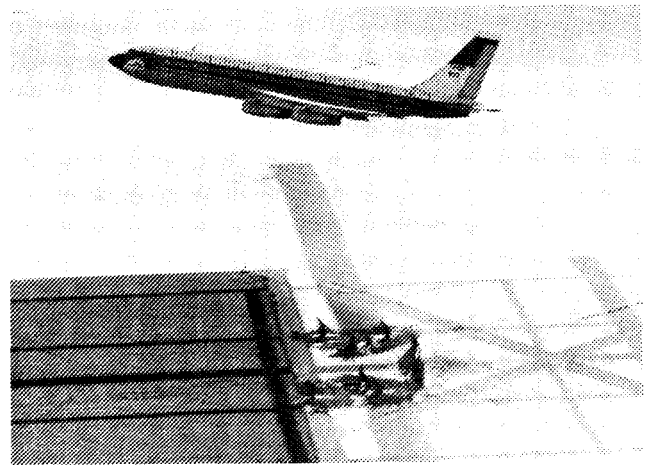
Harney, P.F., J.B. Craft, Jr., and R.G. Johnson, *Remote Control of an Impact Demonstration Vehicle*, NASA TM-85925, 1985.

Curry, R.E., and A.H. Bowers, *Ground-Effect Analysis of a Jet Transport Airplane*, NASA TM-85920, 1985.



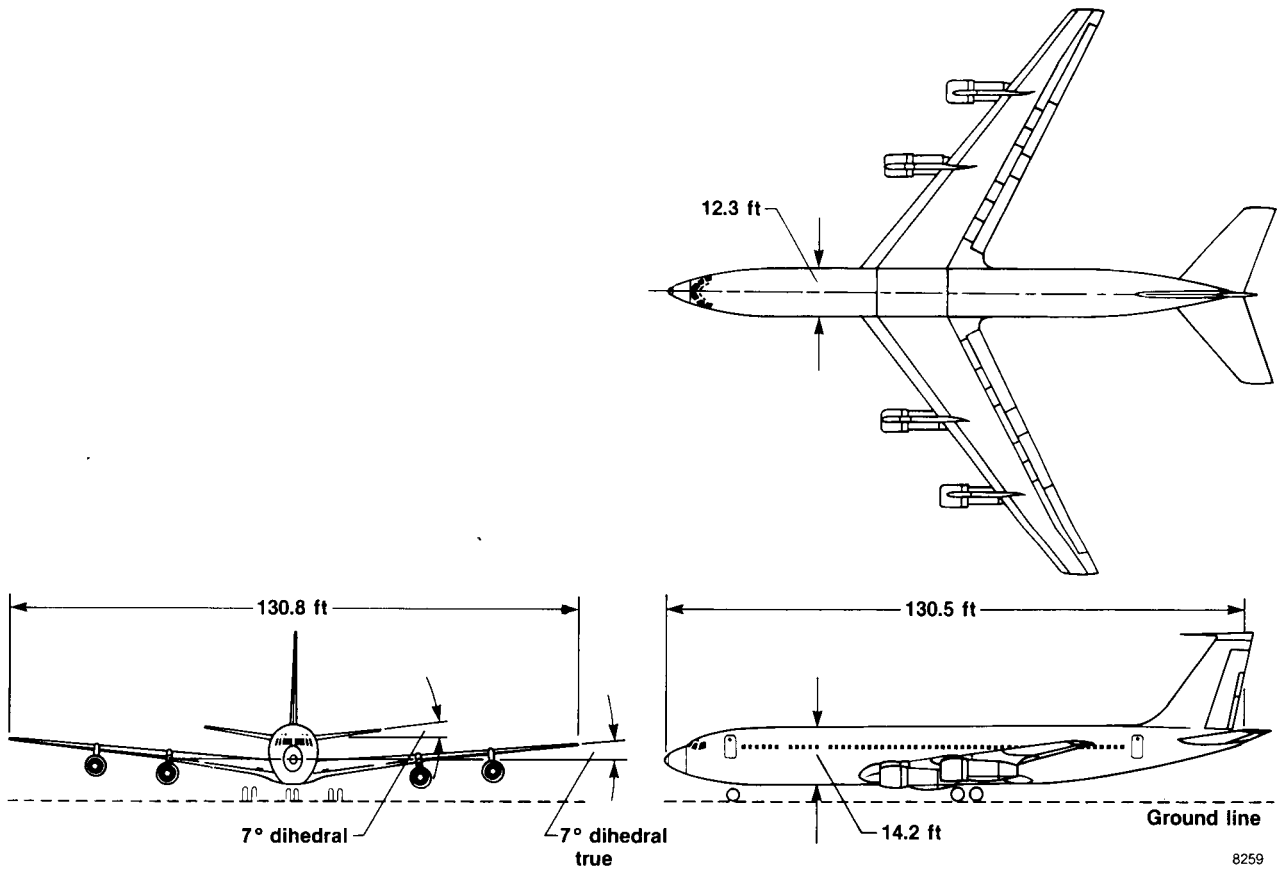
8258

Figure 1. Controlled impact demonstration layout.



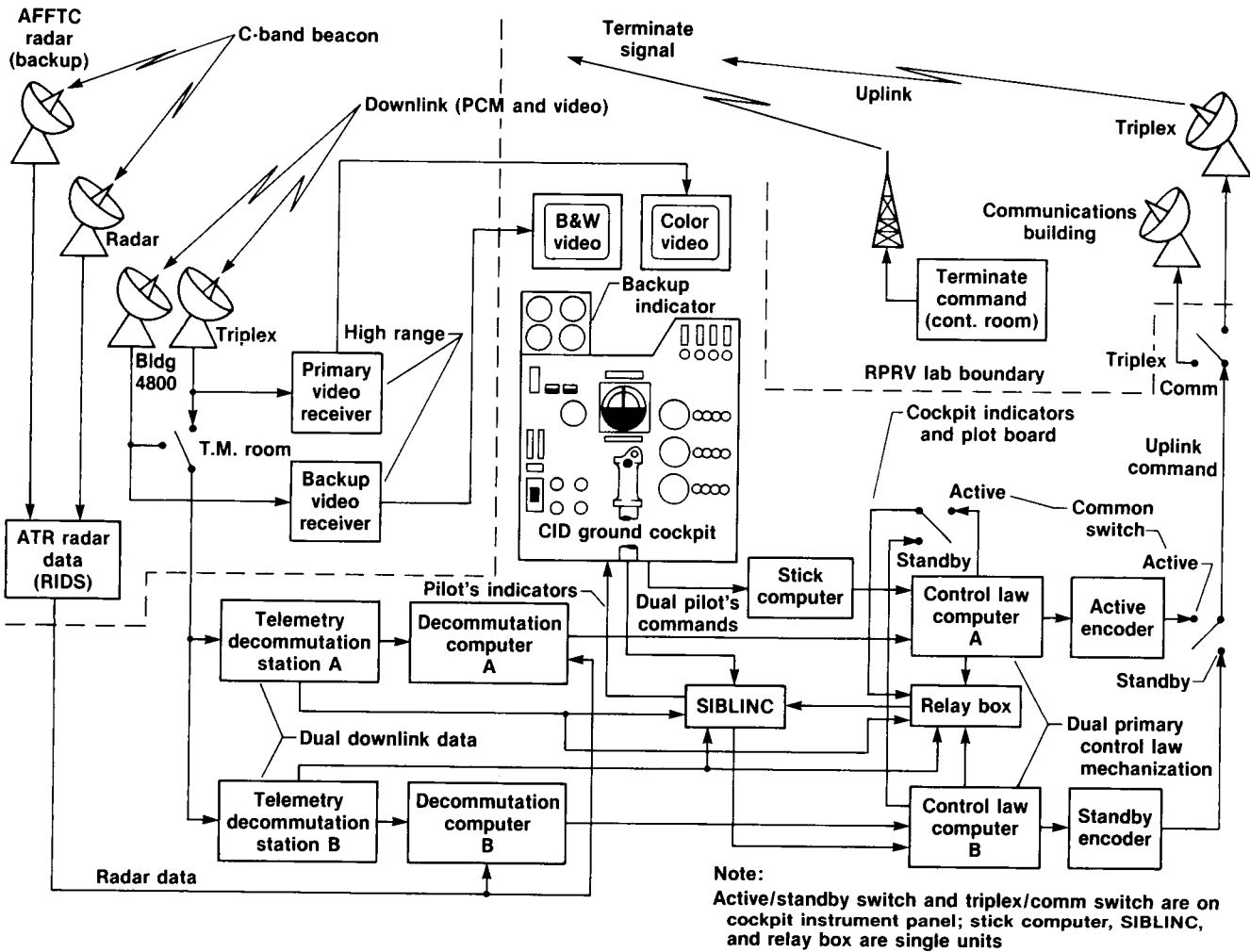
EC84-31672-012

Figure 2. Controlled impact demonstration B-720 aircraft.



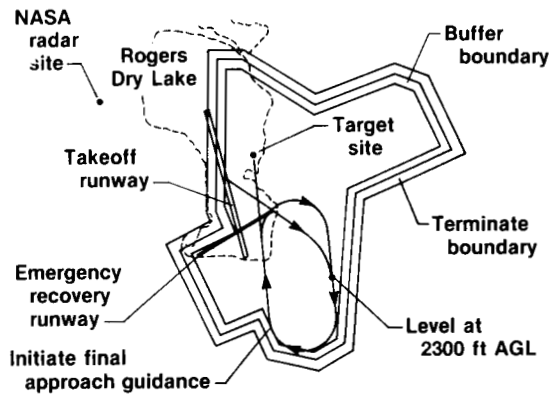
8259

Figure 3. Three-view drawing of B-720 airplane.



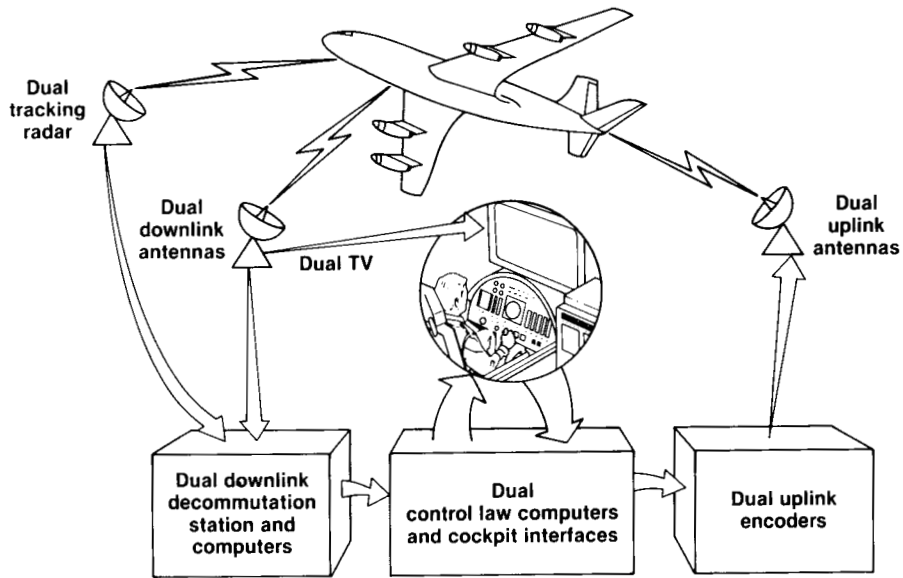
8300

Figure 6. B-720 jet transport controlled impact demonstration ground remotely piloted vehicle control system.



8260

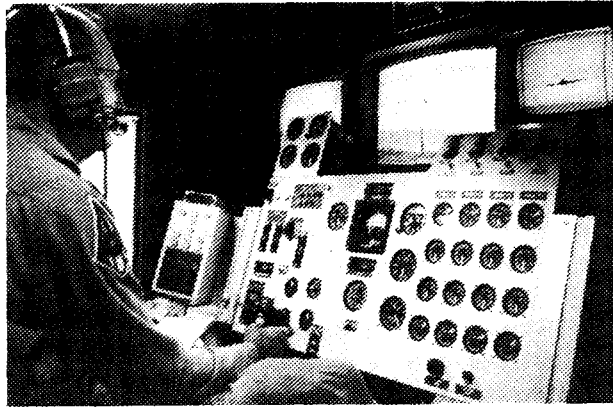
Figure 4. Controlled impact demonstration ground track and sterile area boundary.



8299

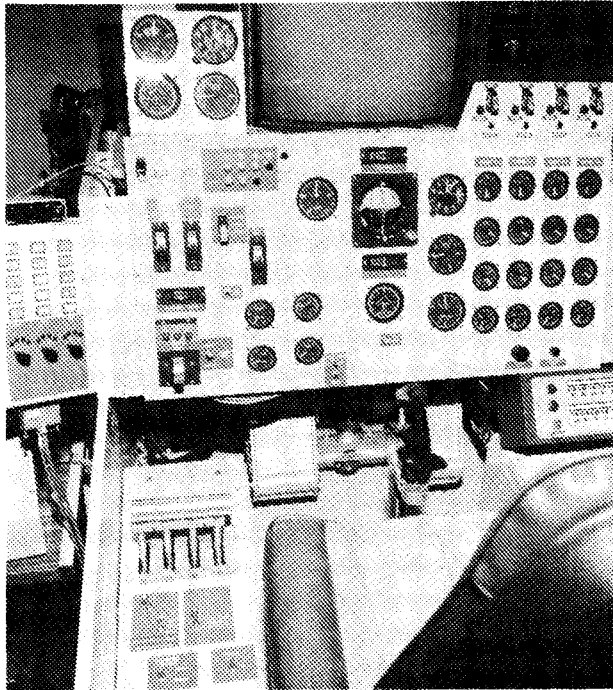
Figure 5. Controlled impact demonstration ground remotely piloted vehicle control system.

ORIGINAL PAGE
BLACK AND WHITE PHOTOGRAPH



ECN-31827

Figure 7. Pilot in remotely piloted vehicle cockpit.



E-40411

Figure 8. Remotely piloted vehicle ground cockpit.

Word	Bits 1 - 10	11	12	13	14	15	16
1	Elevator	Landing gear solenoid enable	Gear up	Gear down	Recorder "A" on	Battery, lights "A" on	Camera "A" on
2	Aileron	No. 1 engine kill	No. 2 engine kill	No. 3 engine kill	No. 4 engine kill	Recorder "A" off	JPL nose camera No. 1 on
3	Rudder	No. 1 engine fire bottle	No. 2 engine fire bottle	No. 3 engine fire bottle	No. 4 engine fire bottle	---	Pneumatic brakes
4	Throttle No. 1	Flap bypass hydraulics	Flap up	Flap down	---	---	---
5	---	JPL cockpit camera No. 2 on	JPL tail camera No. 3 on	---	Throttle servo drive select	JPL camera No. 1 off	Recorder "B" off
6	Left brake	---	---	---	Battery, lights "B" on	Cameras "B" on	Recorder "B" on
7	Right brake	---	JPL camera No. 2 off	JPL camera No. 3 off	---	---	Throttle servo drive select
8	---	Nosewheel steering solenoid	Nosewheel left	Nosewheel right	---	---	---
9	Throttle No. 2	---	---	---	---	---	---

8261

Figure 9. Controlled impact demonstration uplink data format.

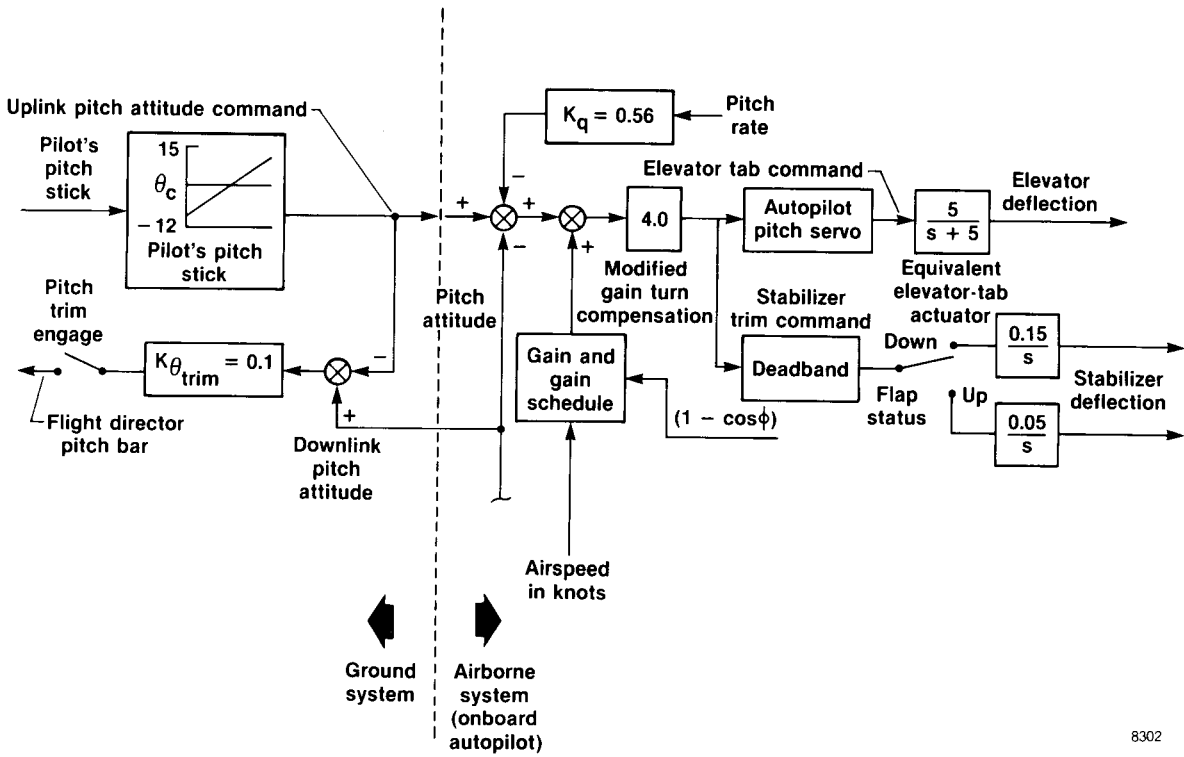
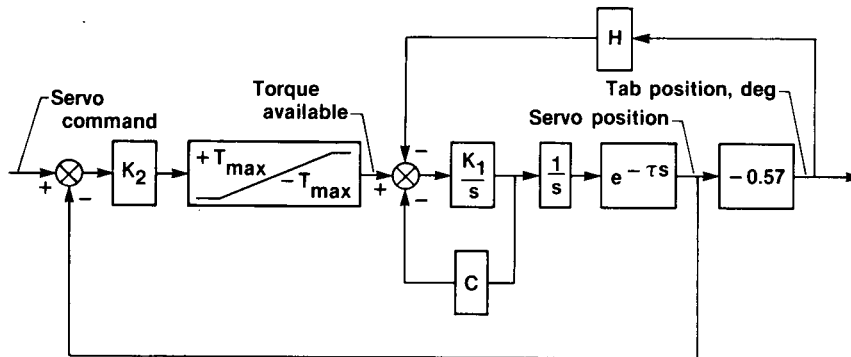


Figure 11. Controlled impact demonstration pitch control system.



$$\tau = 0.25 \text{ sec} \quad K_1 = 7.89$$

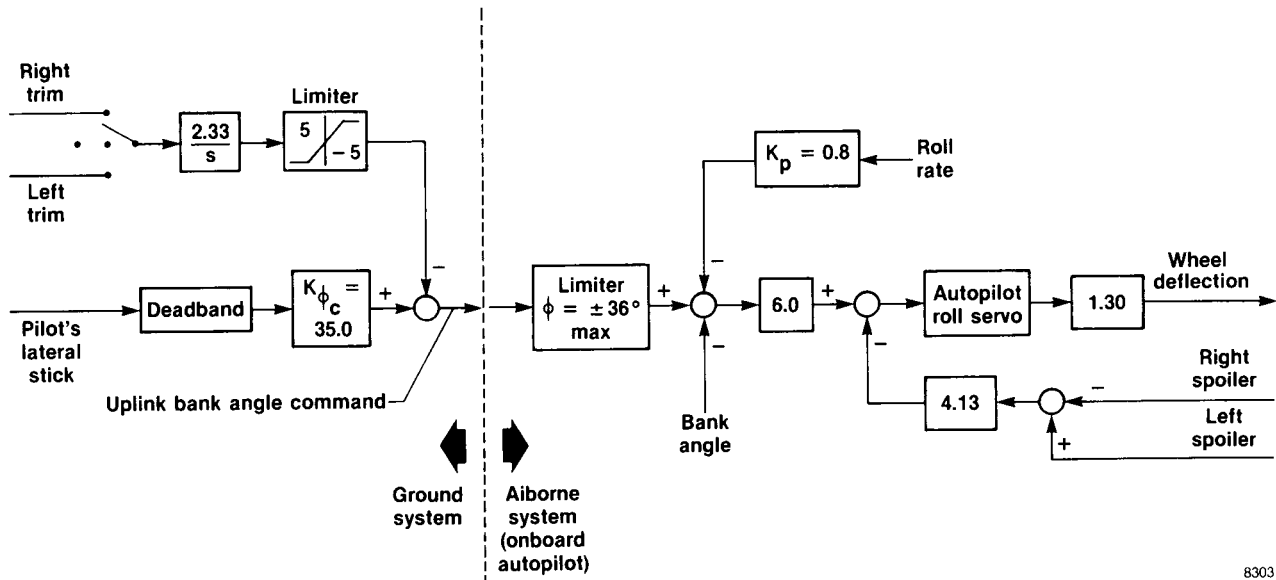
$$T_{\max} = 75 \quad K_2 = 12.7$$

$$C = 1.84$$

$$H = - \left[4.0 + \frac{0.17 V_e^2}{295} \right]$$

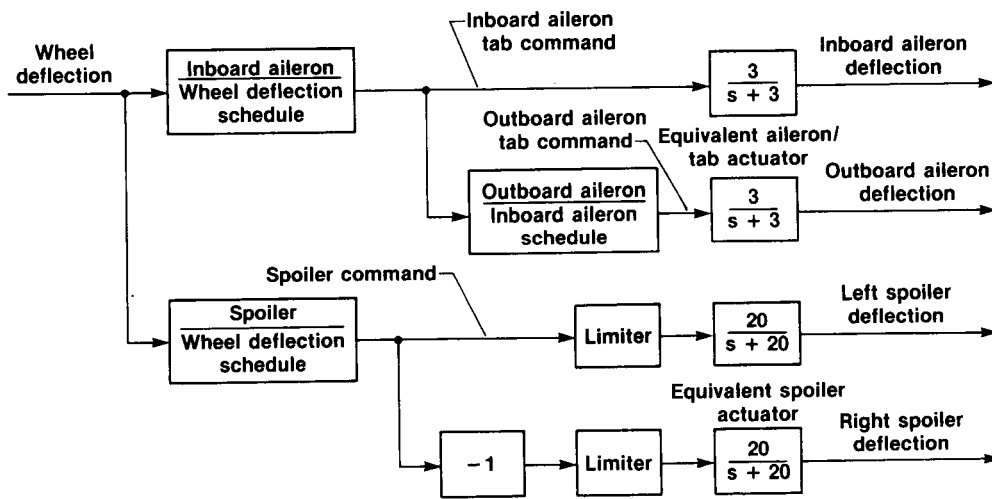
V_e in knots equivalent airspeed

Figure 12. Autopilot elevator servo model.



8303

(a) Control wheel command path.



8304

(b) Aileron and spoiler command path.

Figure 13. Controlled impact demonstration roll control system.

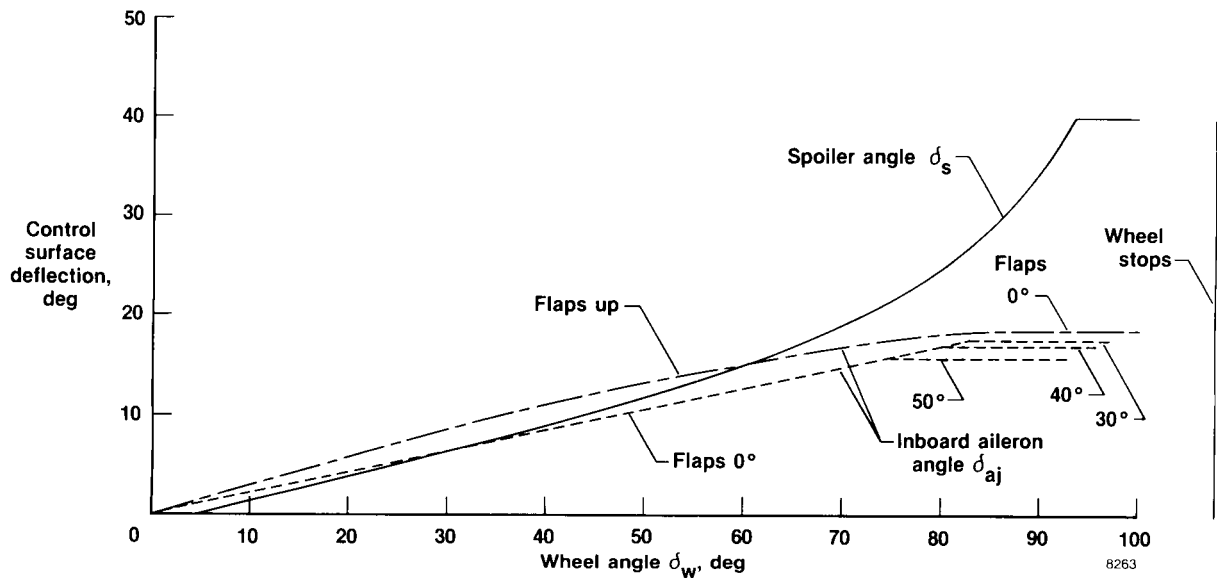


Figure 14. Inboard aileron and spoiler deflection schedules.

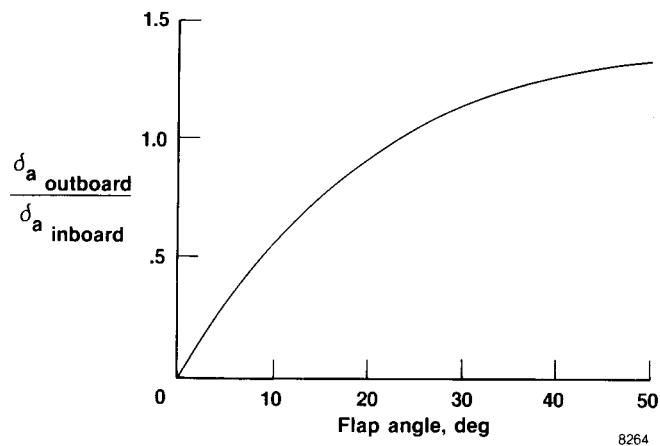


Figure 15. Outboard to inboard aileron schedule.

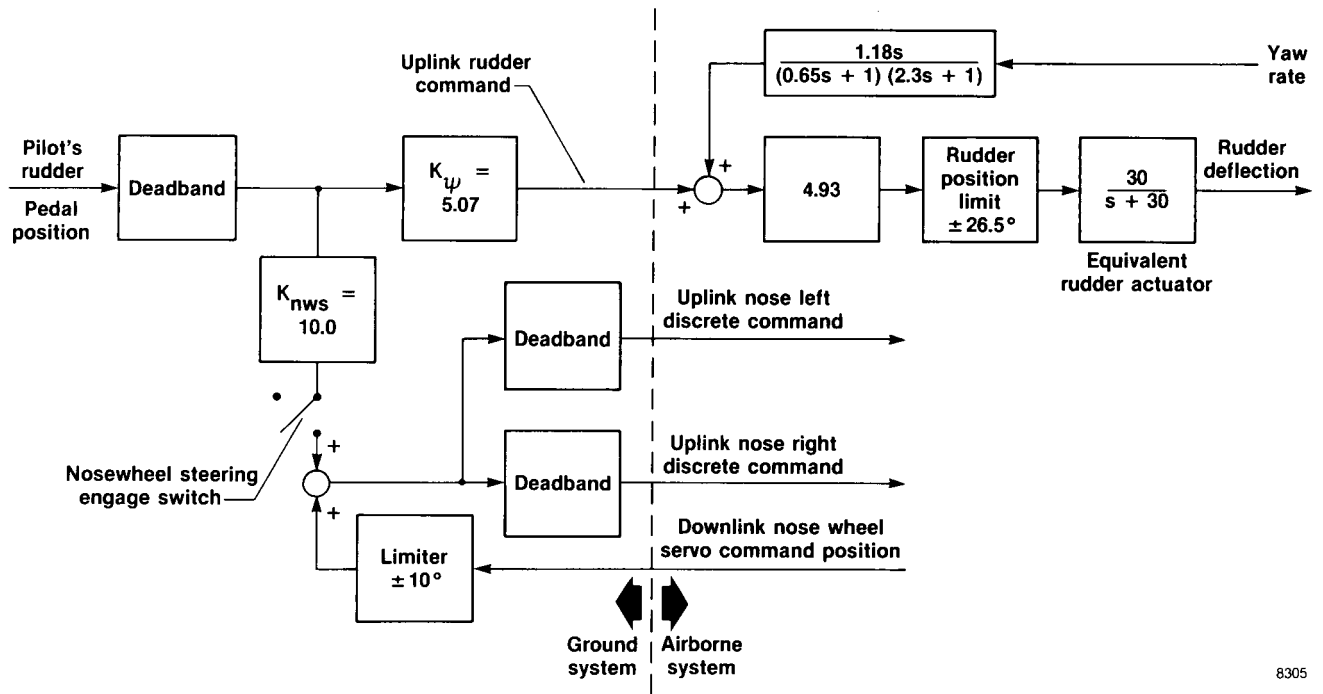


Figure 16. Controlled impact demonstration yaw control system.

8305

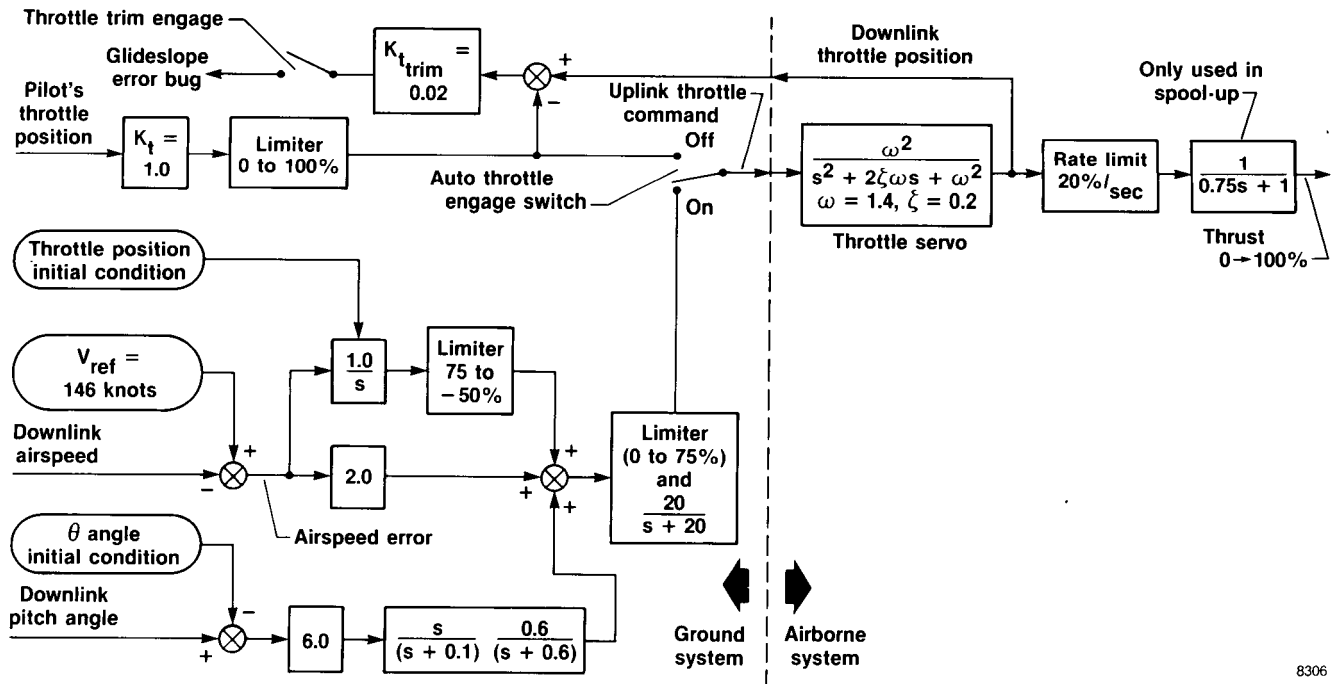
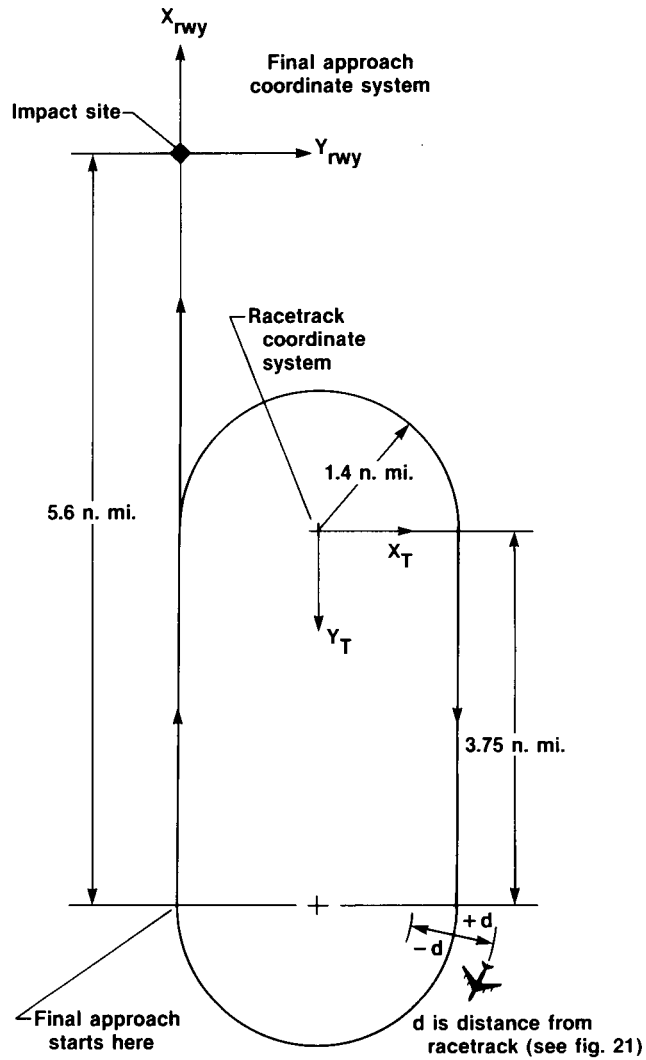


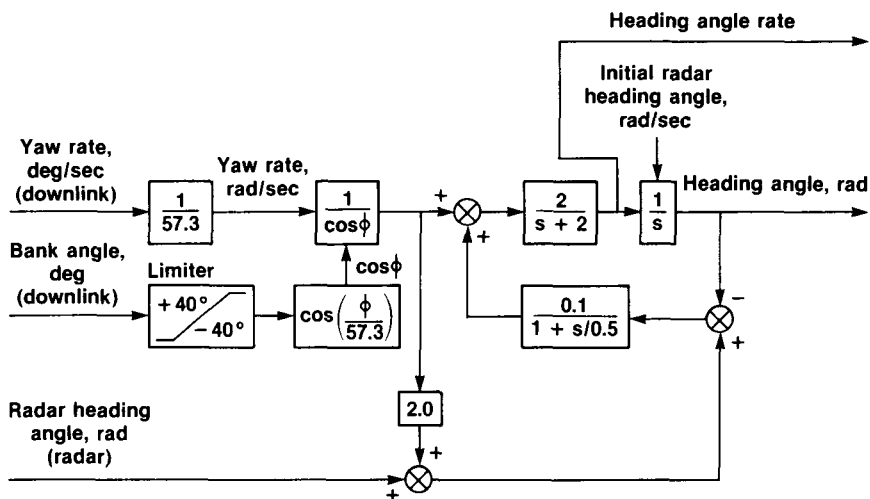
Figure 17. Controlled impact demonstration throttle control system.

8306



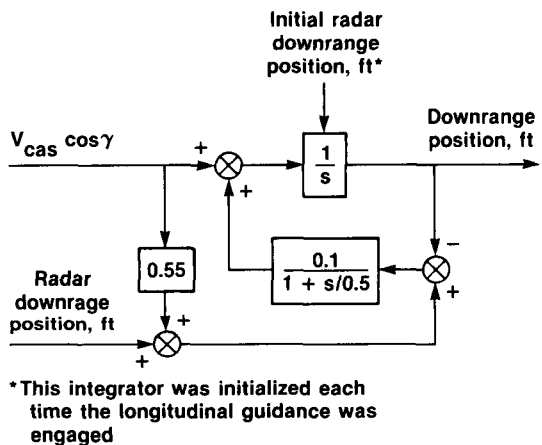
8265

Figure 18. Controlled impact demonstration racetrack and final approach pattern.



8266

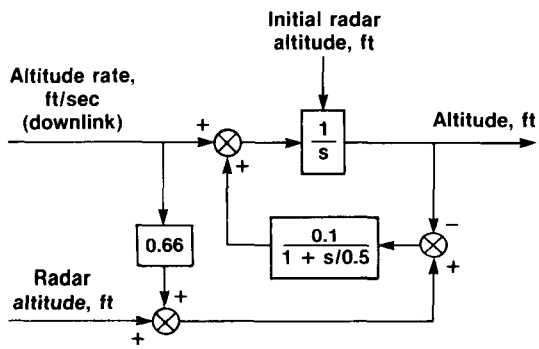
(a) Heading angle calculation.



*This integrator was initialized each time the longitudinal guidance was engaged

8267

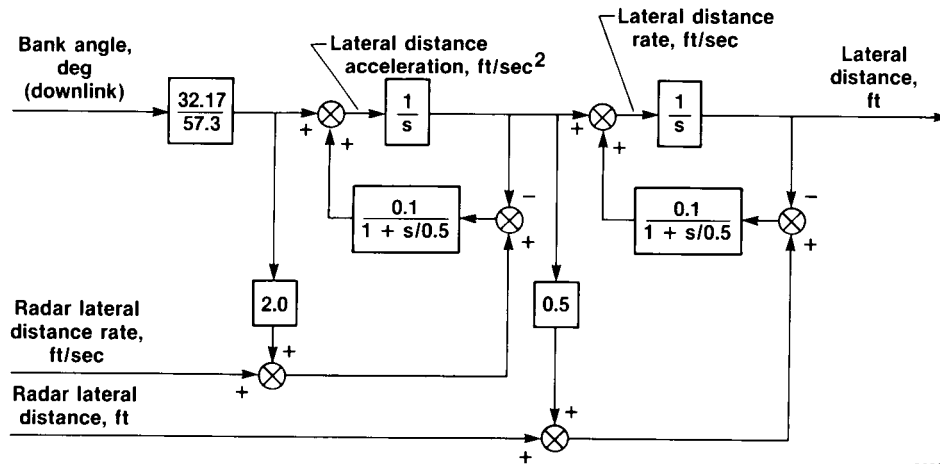
(b) Downrange position calculation.



8268

(c) Altitude calculation.

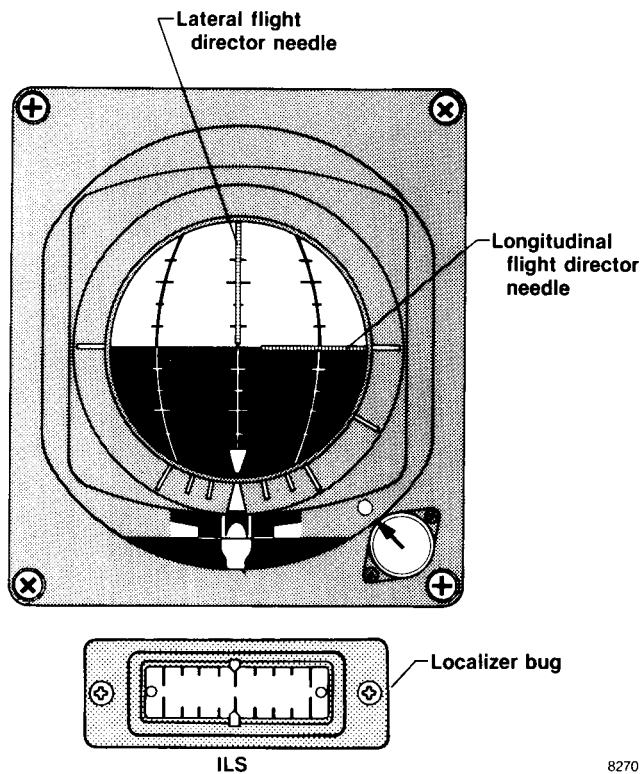
Figure 19. Guidance parameter calculations.



8269

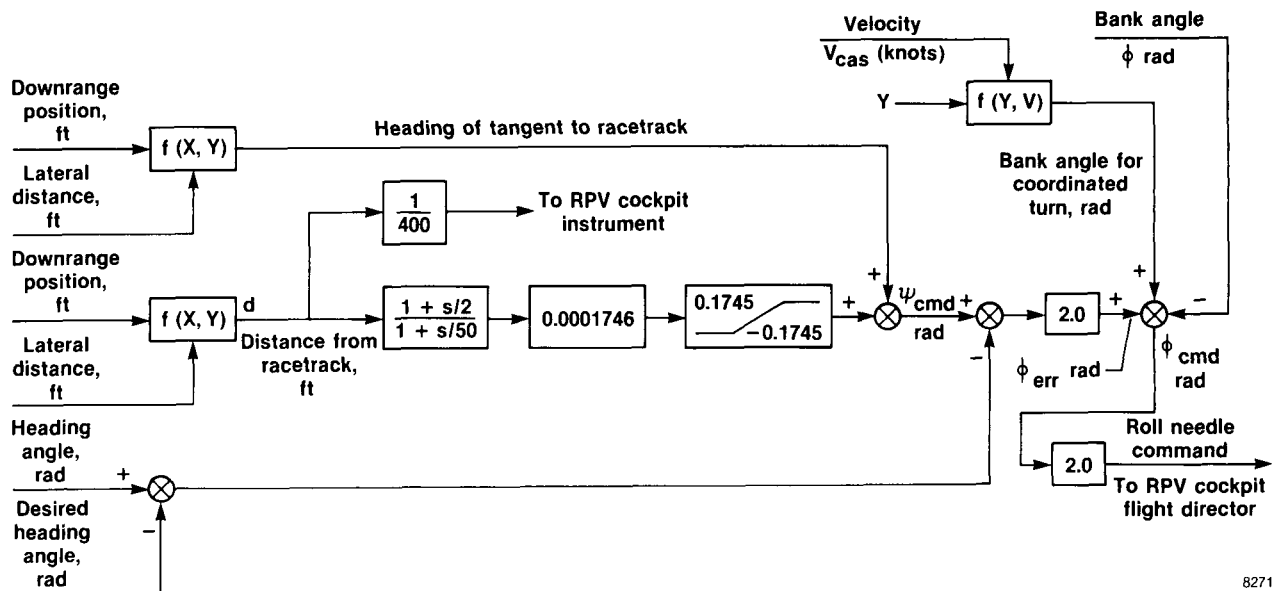
(d) Lateral distance calculation.

Figure 19. Concluded.



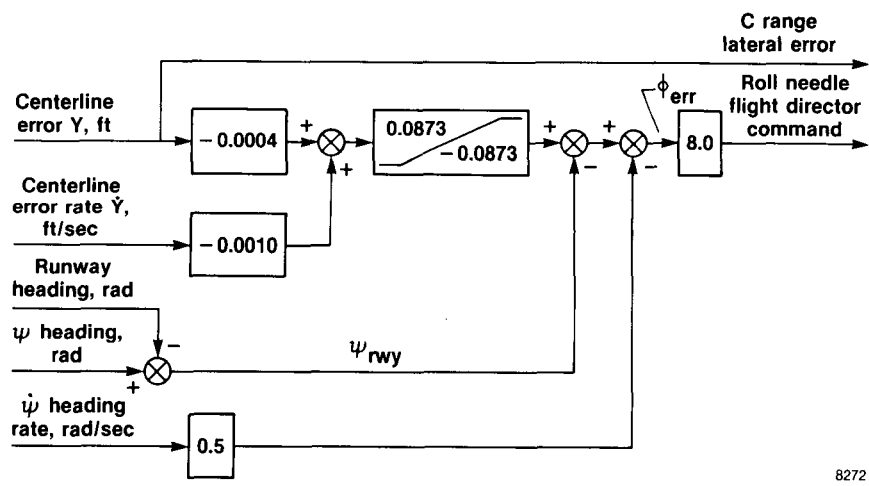
8270

Figure 20. Controlled impact demonstration remotely piloted vehicle cockpit altitude directional indicator.



8271

Figure 21. Lateral racetrack guidance control law.



8272

Figure 22. Lateral final approach control law.

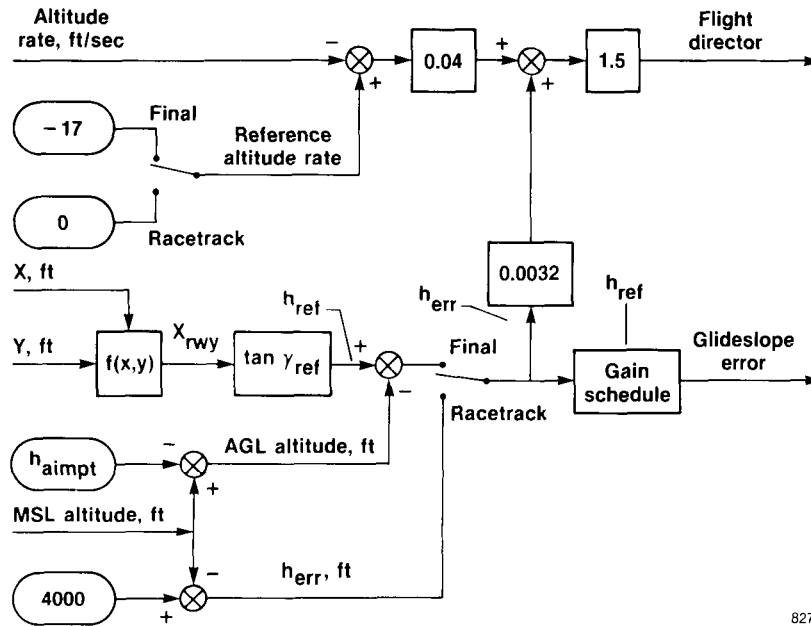


Figure 23. Downrange racetrack and final approach control law.

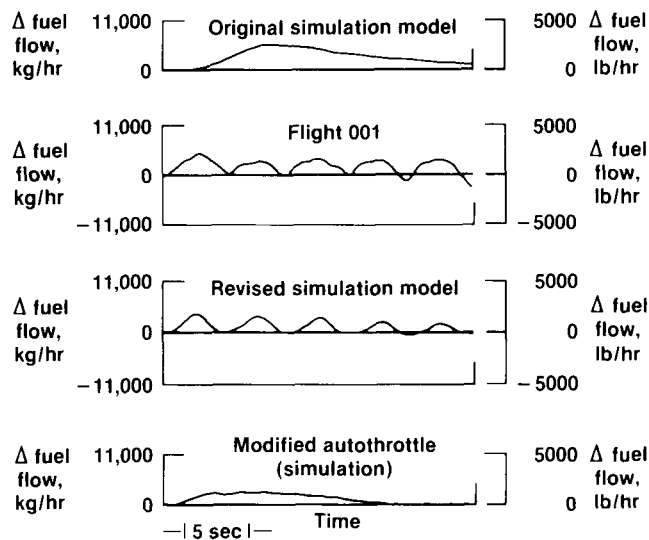
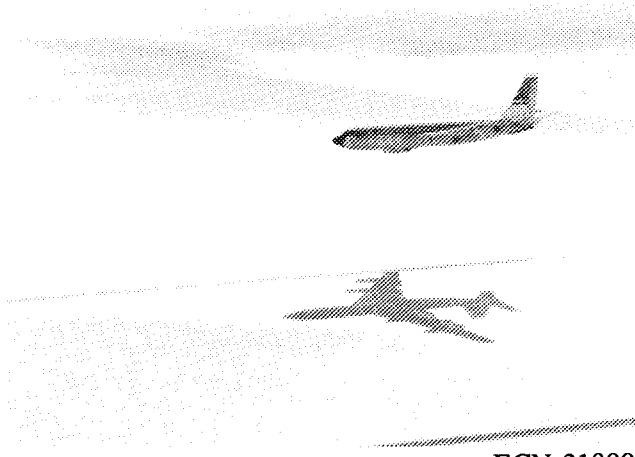


Figure 24. Comparison of flight and simulation engine fuel-flow response to an autothrottle step input.

ORIGINAL PAGE IS
OF POOR QUALITY



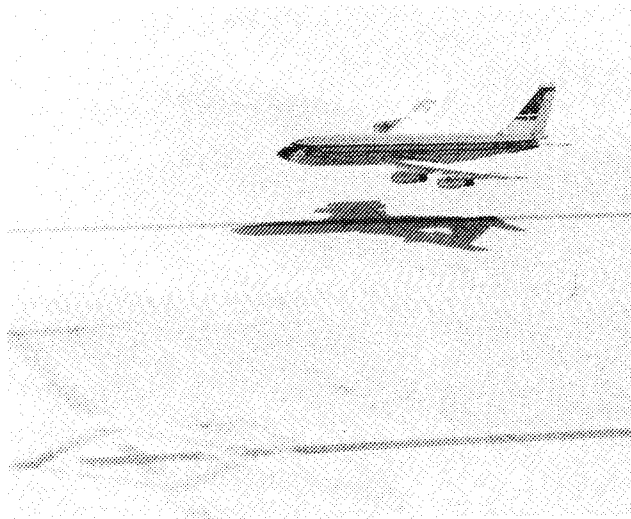
ECN-31800

(a)



ECN-31801

(b)

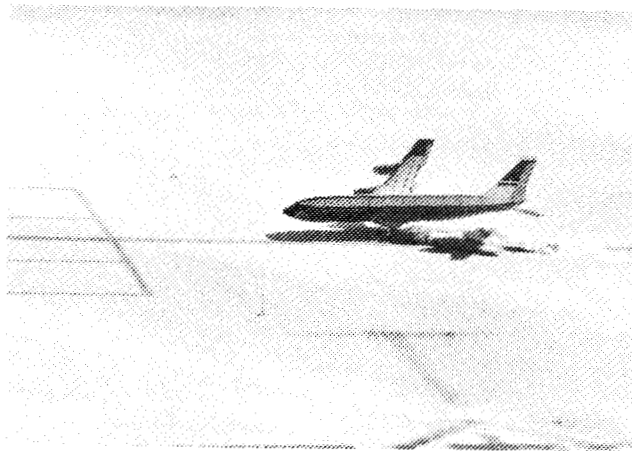


ECN-31802

(c)

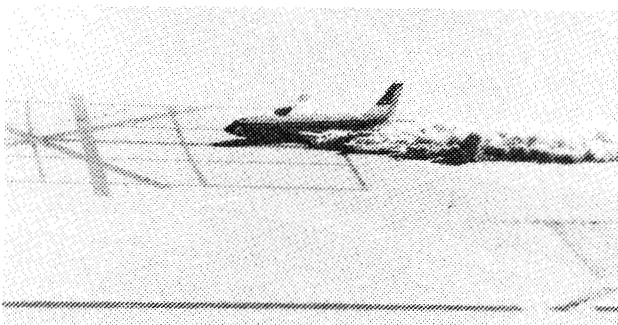
Figure 25. B-720 aircraft approach during impact flight.

ORIGINAL PAGE IS
OF POOR QUALITY



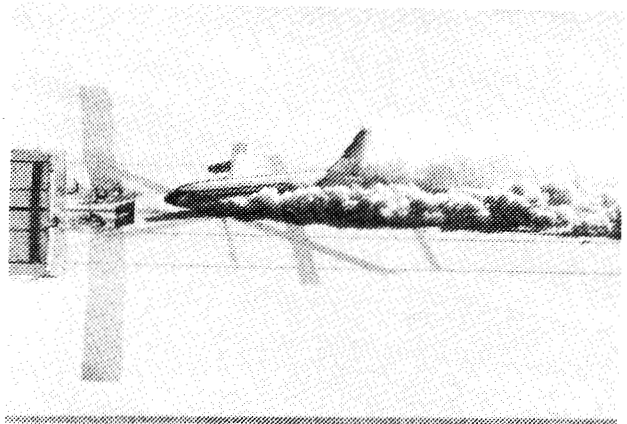
ECN-31803

Figure 26. B-720 aircraft impact.



ECN-31804

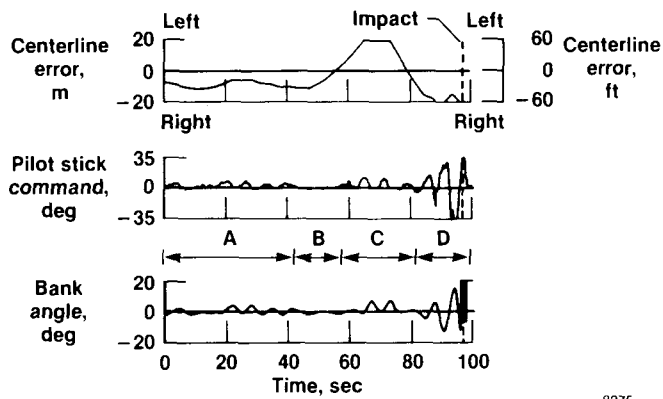
(a)



ECN-31805

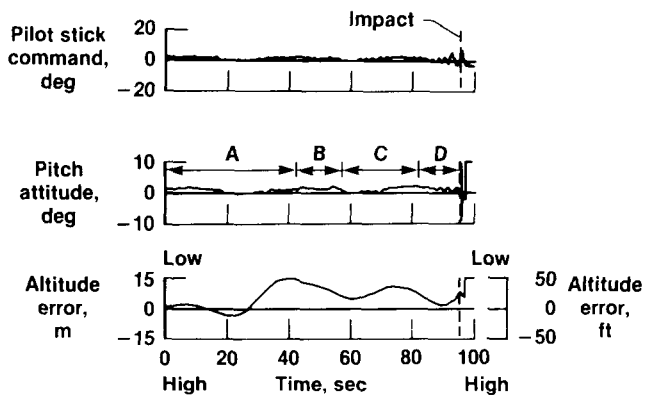
(b)

Figure 27. B-720 aircraft slideout after impact.



8275

Figure 28. Lateral-directional time response from 1630 ft aboveground level to impact.



8276

Figure 29. Longitudinal time response from 1630 ft aboveground level to impact.



Report Documentation Page

1. Report No. NASA TM-4084		2. Government Accession No.		3. Recipient's Catalog No.	
4. Title and Subtitle Flight Test Experience and Controlled Impact of a Remotely Piloted Jet Transport Aircraft				5. Report Date November 1988	
				6. Performing Organization Code	
7. Author(s) Timothy W. Horton and Robert W. Kempel				8. Performing Organization Report No. H-1447	
				10. Work Unit No. RTOP 505-44-24	
9. Performing Organization Name and Address NASA Ames Research Center Dryden Flight Research Facility P.O. Box 273, Edwards, CA 93523-5000				11. Contract or Grant No.	
				13. Type of Report and Period Covered Technical Memorandum	
12. Sponsoring Agency Name and Address National Aeronautics and Space Administration Washington, DC 20546				14. Sponsoring Agency Code	
				15. Supplementary Notes	
16. Abstract The Dryden Flight Research Facility of NASA Ames Research Center (Ames-Dryden) and the Federal Aviation Administration conducted the controlled impact demonstration (CID) program using a large, four-engine, remotely piloted jet transport airplane. Closed-loop primary flight was controlled through the existing onboard PB-20D autopilot which had been modified for the CID program. Uplink commands were sent from a ground-based cockpit and digital computer in conjunction with an up-down telemetry link. These uplink commands were received aboard the airplane and transferred through uplink interface systems to the modified PB-20D autopilot. Both proportional and discrete commands were produced by the ground system. Prior to flight tests, extensive simulation was conducted during the development of ground-based digital control laws. The control laws included primary control, secondary control, and racetrack and final approach guidance. Extensive ground checks were performed on all remotely piloted systems; however, piloted flight tests were the primary method of verification and validation of control law concepts developed from simulation. The design, development, and flight testing of control laws and systems required to accomplish the remotely piloted mission are discussed.					
17. Key Words (Suggested by Author(s)) Remotely piloted transport			18. Distribution Statement Unclassified — Unlimited Subject category 05		
19. Security Classif. (of this report) Unclassified		20. Security Classif. (of this page) Unclassified		21. No. of pages 40	22. Price A03